
Sharpness-Guided Group Relative Policy Optimization via Probability Shaping

Tue Le Linh Ngo Van Trung Le

Abstract

Reinforcement learning with verifiable rewards (RLVR) has become a practical route to improve large language model reasoning, and Group Relative Policy Optimization (GRPO) is a widely used optimizer in this setting. However, RLVR training is typically performed with limited control over generalization. We revisit GRPO through a robustness-based generalization view, where the generalization loss is upper bounded by a combination of the empirical loss and a sharpness surrogate measured by the gradient norm. Building on this perspective, we propose Sharpness-Guided GRPO (GRPO-SG), a simple token-weighted variant of GRPO that downweights tokens likely to cause overly large gradients, reducing sharp updates and stabilizing optimization, thereby improving generalization. Experiments across mathematical reasoning, logic puzzles and tool-augmented question answering show consistent improvements over GRPO, along with smoother gradient-norm trajectories, supporting GRPO-SG as a simple and effective generalization-oriented upgrade to GRPO for RLVR.

1. Introduction

Large language models (LLMs) have recently made major strides on challenging reasoning workloads, especially mathematics and programming, with systems such as OpenAI’s O-series (Jaech et al., 2024), DeepSeek-R1 (Guo et al., 2025), Kimi K2 (Team et al., 2025), and Qwen3 (Yang et al., 2025a) reaching state-of-the-art results. A central driver of these advances is Reinforcement Learning with Verifiable Rewards (RLVR) (Gao et al., 2024; Lambert et al., 2024; Team et al., 2025; Guo et al., 2025; Yang et al., 2025a), which typically performs RL using rule-based outcome signals, for example a binary reward that checks whether the final solution is valid. RLVR offers an effective way to strengthen reasoning by providing stable, task-aligned feedback without relying on expensive human labels or extra

reward models. Among the algorithms used in this setting, Group Relative Policy Optimization (GRPO) (Shao et al., 2024) is widely adopted due to its simplicity and strong empirical performance.

Although recent progress in RLVR has been driven by new algorithms (Yu et al., 2025; Yue et al., 2025; Guan et al., 2025; Zheng et al., 2025; Liu et al., 2026), cross-domain applications (Xue et al., 2025; Liu et al., 2025; Pan et al., 2025), and unexpected empirical observations (Wang et al., 2025; Yue et al., 2025; Zhao et al., 2025; Chandra et al., 2025), most implementations still optimize policy model with limit control over generalization.

In this work, we revisit GRPO through a generalization lens. Theorem 3.3 shows that generalization can be characterized by a robust generalization loss upper bounded by the empirical training loss plus a sharpness term. Using the first-order surrogate in Eq. (15), the sharpness term is measured by the gradient norm. Therefore, smaller gradient norms correspond to less sharp updates, which implies better generalization under this bound. Building on this view, we propose **GRPO-SG (Sharpness-Guided GRPO)**, a simple modification to GRPO that uses token-level probability to control update magnitudes. Concretely, GRPO-SG assigns each token a weight given by a monotone function of the model’s own token probability in Eq. (19). These weights are integrated into the standard GRPO surrogate, so the optimization downweights tokens that would otherwise induce sharp, unstable gradients, while preserving learning signal on tokens that the policy is confident about and repeatedly relies on during reasoning. Under the generalization bound above, the objective is direct: use token weights to reduce the gradient-norm term in Eq. (15), thereby improving generalization.

Experiments across diverse settings including logic puzzles, mathematical reasoning, and agentic QA confirm that Sharpness-Guided GRPO consistently outperforms GRPO. In particular, across all these RLVR settings, GRPO-SG delivers substantial gains: on the K&K logic puzzles benchmark, Qwen2.5-3B improves from **0.39** to **0.63** (Table 3); in agentic multi-hop QA, exact-match accuracy nearly doubles from **13.84** to **27.29** (Table 2); and on math benchmarks including OlympiadBench and Minerva, we observe average improvements of **+6–10%** (Table 1). Beyond accu-

. Correspondence to: Tue Le <tue209003@gmail.com>.

racy, GRPO-SG yields smoother gradient-norm trajectories and more stable training (Figure 1), consistent with the sharpness-control mechanism.

In summary, this paper makes three main contributions:

- We provide a generalization view of GRPO by linking RLVR training to a robust generalization objective and its sharpness surrogate.
- Guided by this view, we propose GRPO-SG, a simple GRPO variant that applies probability-shaped token weights to regulate per-token update magnitude and reduce sharpness.
- We validate GRPO-SG across diverse RLVR benchmarks, showing consistent gains over GRPO together with smoother gradient-norm trajectories and more stable training.

2. Background

2.1. Large Language Models

Most **Large Language Models (LLMs)** adopt a transformer decoder-only architecture (Vaswani et al., 2017), parameterized by $\theta \in \mathbb{R}^d$ and denoted as π_θ . The basic unit of an LLM is the token, which may correspond to a word, subword, or character, and is selected from a finite vocabulary $\mathcal{V} = \{v^1, \dots, v^N\}$ of size N . Given a prompt q , the model generates a sequence of tokens $o = (o_1, \dots, o_T)$ autoregressively. At each step t , the model produces a distribution over \mathcal{V} conditioned on q and the previously generated tokens $o_{<t}$, from which the next token is sampled:

$$o_t \sim \pi_\theta(\cdot | q, o_{<t}). \quad (1)$$

This process continues until an end-of-sequence (EOS) token is produced or the sequence length reaches a predefined maximum t_{\max} .

While pretrained and supervised fine-tuned LLMs achieve fluency, practical applications often require alignment with human preferences or reasoning ability, which is not easily captured by likelihood training alone. To address this, one may introduce a reward function $r(q, o)$ that quantifies the quality of a generated sequence o given prompt q . The learning problem can then be cast as reinforcement learning, where the prompt q represents the state, each generated token is an action, and the full output o yields a terminal reward. Accordingly, the optimization objective is formulated as: $\max_{\theta} \mathbb{E}_{q \sim \mathcal{Q}, o \sim \pi_\theta(\cdot | q)} [r(q, o)]$, where \mathcal{Q} denotes a dataset of prompts.

2.2. Reinforcement Learning with Verifiable Rewards (RLVR)

Reinforcement Learning with Verifiable Rewards (RLVR) (Gao et al., 2024; Lambert et al., 2024; Team et al., 2025; Guo et al., 2025; Yang et al., 2025a) provides a framework for optimizing LLMs in domains where correctness can be *deterministically verified*. Typical applications include code generation validated by unit tests, mathematical problem solving with symbolic checkers, and factual QA with exact-match rules or programmatic validators. Unlike preference-based reinforcement learning, RLVR leverages a predefined verifier to produce a reward without requiring human labels. Formally, given a dataset of prompts \mathcal{D} , a policy π_θ , and a frozen reference model π_{ref} , the objective is:

$$\max_{\theta} \mathbb{E}_{q \sim \mathcal{Q}, o \sim \pi_\theta(\cdot | q)} [R_\phi(q, o)] - \beta \mathbb{D}_{\text{KL}}[\pi_\theta(o | q) \| \pi_{\text{ref}}(o | q)], \quad (2)$$

where R_ϕ is the verifiable reward function and β controls the KL regularization. A typical verifiable reward function is defined as:

$$R_\phi(q, o) = \begin{cases} 1 & \text{if match}(o, o_g), \\ -1 & \text{otherwise,} \end{cases} \quad (3)$$

where o_g is the ground-truth answer and $\text{match}(\cdot, \cdot) \in \{0, 1\}$ indicates whether the generated output matches. More generally, R_ϕ may be graded (e.g., partial credit, length penalty, latency) while remaining *verifiable* by rule-based approaches (Wang et al., 2024) or model-based verifiers (Ma et al., 2025).

In summary, RLVR provides a principled setting where optimization is guided by *verifiable correctness*, making it a natural foundation for training reasoning-oriented LLMs.

2.3. Group Relative Policy Optimization (GRPO)

Group Relative Policy Optimization (GRPO), first introduced by Shao et al. (2024), is a policy-gradient algorithm widely used for optimizing the objective in Eq. (2). Unlike the popular PPO algorithm (Schulman et al., 2017), which requires training an additional value function alongside the LLM, GRPO removes the dependency on an explicit value model. Instead, it estimates advantages by *normalizing rewards within a group* of sampled responses to the same prompt. Specifically, for a prompt q with G sampled responses $\{o_i\}_{i=1}^G$ and associated scalar rewards $\{r_i\}_{i=1}^G$, GRPO defines a group-normalized advantage as:

$$\hat{A}_{i,t} = \frac{r_i - \text{mean}(\{r_j\}_{j=1}^G)}{\text{std}(\{r_j\}_{j=1}^G)}, \quad (4)$$

The effectiveness of the above normalization method can be interpreted through the lens of reward shaping: by emphasizing relative differences among candidate outputs for

the same prompt, it strengthens the stability of the gradient signal and maintains its reliability, even under sparse reward conditions (Hu et al., 2020). In this study, we employ a variant of GRPO to optimize the policy model π_θ . The optimization objective of GRPO can be expressed:

$$\begin{aligned} \mathcal{J}_{\text{GRPO}}(\theta) = & \mathbb{E}[q \sim \mathcal{Q}, \{o_i\}_{i=1}^G \sim \pi_{\theta_{\text{old}}}(O | q)] \\ & \frac{1}{\sum_{i=1}^G |o_i|} \sum_{i=1}^G \sum_{t=1}^{|o_i|} \left\{ \min(r_{i,t}(\theta) \hat{A}_{i,t}, \right. \\ & \left. \text{clip}(r_{i,t}(\theta), 1 - \epsilon_l, 1 + \epsilon_h) \hat{A}_{i,t}) \right. \\ & \left. - \beta \mathbb{D}_{\text{KL}}[\pi_\theta \| \pi_{\text{ref}}] \right\}, \end{aligned} \quad (5)$$

where $r_{i,t}(\theta) = \frac{\pi_\theta(o_{i,t} | q, o_{i,<t})}{\pi_{\theta_{\text{old}}}(o_{i,t} | q, o_{i,<t})}$ is the importance sampling ratio and the KL divergence term. $\pi_{\theta_{\text{old}}}$ denotes the policy used to sample responses, π_{ref} is a frozen reference model, and ϵ_l, ϵ_h are the PPO-style clipping threshold hyperparameters and β controls KL regularization.

3. Methodology

3.1. A generalization view of GRPO

We investigate the generalization ability of RL reasoning approaches, such as GRPO. Let \mathcal{Q} denote the distribution to generate questions q (i.e., $q \sim \mathcal{Q}$). Given $q \sim \mathcal{Q}$, we further denote $\pi_*(\cdot | q)$ as the *oracle distribution* to generate ground-truth perfect solutions $o \sim \pi_*(\cdot | q)$. Given a parameterized LLM π_θ , we want to train it as

$$\begin{aligned} \max_{\theta} \mathbb{E}_{q \sim \mathcal{Q}, o \sim \pi_*(\cdot | q)} & \left[\frac{1}{|o|} \sum_{t=1}^{|o|} r^*([q, o_{<t}], o_t) \pi_\theta(o_t) \right] \\ & - \beta \mathbb{D}_{\text{KL}}(\pi_\theta \| \pi_{\text{ref}}) \equiv \\ \max_{\theta} \mathbb{E}_{q \sim \mathcal{Q}} & \left[\frac{1}{|o|} \sum_{t=1}^{|o|} \mathbb{E}_{o_{\leq t} \sim \pi_*^t(\cdot | q)} [r^*([q, o_{<t}], o_t) \pi_\theta(o_t)] \right] \\ & - \beta \mathbb{D}_{\text{KL}}(\pi_\theta \| \pi_{\text{ref}}), \end{aligned} \quad (6)$$

where the regularization term $\mathbb{D}_{\text{KL}}(\pi_\theta \| \pi_{\text{ref}})$ preserves π_θ from π_{ref} , we denote $\pi_\theta(o_t) = \pi_\theta(o_t | q, o_{<t})$, and $\pi_*^t(\cdot | q)$ is the marginal of $\pi_*(\cdot | q)$ over $o_{\leq t}$. Here we note that $r^*([q, o_{<t}], o_t)$ is the optimal reward function obtained from the oracle distribution $\pi_*(\cdot | q)$. Moreover, $r^*([q, o_{<t}], o_t)$ means that given $[q, o_{<t}]$, what the reward to generate o_t is if $o_t \sim \pi_*(o_t | q, o_{<t})$. Specifically, the connection between the oracle distribution π_* and its opti-

mal reward r_* is as follows:

$$\begin{aligned} \pi_* = & \operatorname{argmax}_{\pi} \left\{ \mathbb{E}_q \left[\sum_{t=1}^{|o|} \mathbb{E}_{o_t \sim \pi(\cdot | q, o_{<t})} [r_*([q, o_{<t}], o_t)] \right] \right. \\ & \left. - \lambda \sum_{t=1}^{|o|} D_f(\pi(\cdot | q, o_{<t}) \| \pi_{\text{old}}(\cdot | q, o_{<t})) \right\}, \end{aligned} \quad (7)$$

where f is a convex function. We note that Eq. (21) indicates that π_* is the distribution that maximizes the reward $r_*([q, o_{<t}], o_t)$ when $o_t \sim \pi_*(\cdot | q, o_{<t})$. With some manipulations, we reach the optimal solution in the following lemma.

Lemma 3.1. *The optimal solution of (21) is*

$$r^*([q, o_{<t}], o_t) = \lambda f' \left(\frac{\pi_*(o_t)}{\pi_{\text{old}}(o_t)} \right) + \text{const.} \quad (8)$$

Moreover, by choosing $f(t) = \lambda^{-1} \int_0^t \frac{\omega(x \pi_{\text{old}}(o_t))}{\pi_{\text{old}}(o_t)} dx$ for some convex function $\omega(\cdot)$ ¹, we have

$$f'(t) = \lambda^{-1} \frac{\omega(t \pi_{\text{old}}(o_t))}{\pi_{\text{old}}(o_t)}$$

Finally, by choosing $t = \frac{\pi_*(o_t)}{\pi_{\text{old}}(o_t)}$, we reach

$$\begin{aligned} r_*([q, o_{<t}], o_t) &= \lambda f' \left(\frac{\pi(o_t)}{\pi_{\text{old}}(o_t)} \right) + \text{const} \\ &= \frac{\omega(\pi_*(o_t))}{\pi_{\text{old}}(o_t)} + \text{const}. \end{aligned}$$

The optimization problem in (6) now becomes

$$\begin{aligned} \max_{\theta} \mathbb{E}_{\mathcal{Q}} & \left[\frac{1}{|o|} \sum_{t=1}^{|o|} \mathbb{E}_{o_{\leq t} \sim \pi_*^t(\cdot | q)} \left[\omega(\pi_*(o_t)) \frac{\pi_\theta(o_t)}{\pi_{\text{old}}(o_t)} \right] \right] \\ & - \beta \mathbb{D}_{\text{KL}}(\pi_\theta \| \pi_{\text{ref}}). \end{aligned} \quad (9)$$

In the following theorem, hinted by GRPO, we change the trajectories $o_{\leq t}$ sampled from the oracle distribution π_*^t to those sampled from the old (checkpoint) policy π_{old} , which introduces the shift terms.

Theorem 3.2. *Given a checkpoint LLM $\pi_{\text{old}}(\cdot | q)$, we can upper-bound the objective function in (23) by*

$$\begin{aligned} \mathbb{E}_{q \sim \mathcal{Q}} & \left[\frac{1}{|o|} \sum_{t=1}^{|o|} \mathbb{E}_{o_{\leq t} \sim \pi_{\text{old}}^t(\cdot | q)} \left[\omega(\pi_\theta(o_t)) \frac{\pi_\theta(o_t)}{\pi_{\text{old}}(o_t)} \right] \right] \\ & + \mathbb{E}_{q \sim \mathcal{Q}} \left[\frac{1}{|o|} \sum_{t=1}^{|o|} \left\{ d(\pi_{\text{old}}^t, \pi_*^t) + d'(\pi_\theta^t, \pi_*^t) \right\} \right] \\ & - \beta \mathbb{D}_{\text{KL}}(\pi_\theta \| \pi_{\text{ref}}), \end{aligned} \quad (10)$$

¹This ensures that f defined above is a convex function

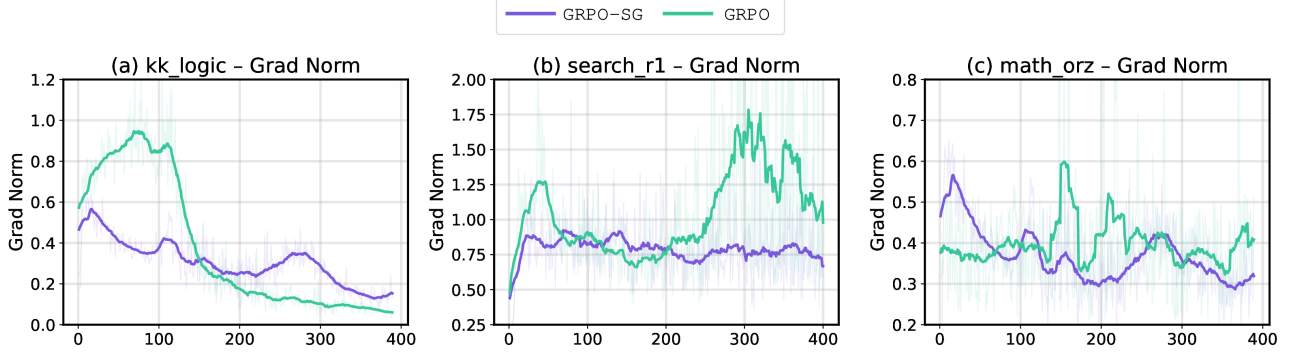


Figure 1. Gradient norm trajectories during training under GRPO vs. GRPO-SG across three RLVR settings. GRPO-SG consistently exhibits lower variability and fewer spikes than GRPO, consistent with reduced sharpness in Eq. (15) and the bound in Eq. (16).

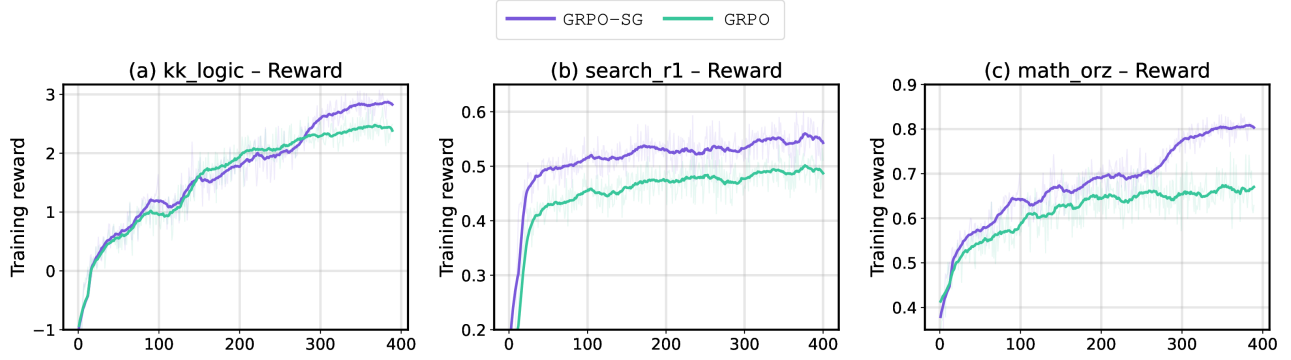


Figure 2. Training reward trajectories during training under GRPO vs. GRPO-SG across three RLVR settings. GRPO-SG achieves higher reward while also exhibiting lower sharpness as reflected by gradient norms.

where d and d' are divergences between two distributions. More details can be found in Appendix D.2.

Ignoring the shift terms, we can rewrite the OP in (10) as

$$\begin{aligned} & \max_{\theta} \mathbb{E}_{\mathcal{Q}} \left[\frac{1}{|o|} \sum_{t=1}^{|o|} \mathbb{E}_{o_{\leq t} \sim \pi_{old}^t(\cdot|q)} \left[\omega(\pi_{\theta}(o_t)) \frac{\pi_{\theta}(o_t)}{\pi_{old}(o_t)} \right] \right] \\ & - \beta \mathbb{D}_{\text{KL}}(\pi_{\theta} \| \pi_{ref}) \equiv \\ & \max_{\theta} \left[\mathbb{E}_{\mathcal{Q}, o \sim \pi_{old}(\cdot|q)} \left[\frac{1}{|o|} \sum_{t=1}^{|o|} \omega(\pi_{\theta}(o_t)) \frac{\pi_{\theta}(o_t)}{\pi_{old}(o_t)} \right] \right] \\ & - \beta \mathbb{D}_{\text{KL}}(\pi_{\theta} \| \pi_{ref}). \end{aligned} \quad (11)$$

We further rewrite (11) using multiple $o_{1:G} \stackrel{iid}{\sim} \pi_{old}(\cdot|q)$:

$$\begin{aligned} & \max_{\theta} \mathbb{E}_{q \sim \mathcal{Q}, o_{1:G} \sim \pi_{old}(\cdot|q)} \left[\frac{1}{\sum_{i=1}^G |o_i|} \sum_{i=1}^G \sum_{t=1}^{|o_i|} \omega(\pi_{\theta}(o_{i,t})) \right. \\ & \left. \frac{\pi_{\theta}(o_{i,t})}{\pi_{old}(o_{i,t})} \right] - \beta \mathbb{D}_{\text{KL}}(\pi_{\theta} \| \pi_{ref}). \end{aligned} \quad (12)$$

We denote $r_{\theta}(o_{i,t}) = \frac{\pi_{\theta}(o_{i,t})}{\pi_{old}(o_{i,t})}$. Moreover, inspired by PPO and GRPO, to encourage learning and unlearning from both

well-qualified and unqualified responses o_i by using the advantage function $\hat{A}_{i,t}$, we adopt the optimization problem in (12) as

$$\begin{aligned} & \max_{\theta} \mathbb{E}_{q \sim \mathcal{Q}, o_{1:G} \sim \pi_{old}(\cdot|q)} \left[\frac{1}{\sum_{i=1}^G |o_i|} \sum_{i=1}^G \sum_{t=1}^{|o_i|} \mathcal{J}(o_{i,t}) \right] \\ & - \beta \mathbb{D}_{\text{KL}}(\pi_{\theta} \| \pi_{ref}), \end{aligned} \quad (13)$$

where we have defined

$$\begin{aligned} & \mathcal{J}(o_{i,t}) := \min \left\{ \omega(\pi_{\theta}(o_{i,t})) r_{\theta}(o_{i,t}) \hat{A}_{i,t}, \right. \\ & \left. \text{clip}(\omega(\pi_{\theta}(o_{i,t})) r_{\theta}(o_{i,t}), 1 - \epsilon_l, 1 + \epsilon_h) \hat{A}_{i,t} \right\}. \end{aligned}$$

For the OP in (13), we need to optimize the generalization loss over the joined distribution \mathcal{D} including samples (q, o_1, \dots, o_G) with the pdf $p(q, o_{1:G})$, defined as $\mathcal{Q}(q) \prod_{i=1}^G \pi_{old}(o_i | q)$. However, in the actual training, we only rely on a finite training set of $\mathcal{S} = [(q_k, o_{k1}, \dots, o_{kG})]_{k=1, \dots, N}$ to train an LLM model. This introduces a gap between the generalization and empirical losses. Let us denote *generalization loss* over \mathcal{D} and the

empirical loss over the training set \mathcal{S} as $\mathcal{L}_{\mathcal{D}}(\pi_{\theta})$ and $\mathcal{L}_{\mathcal{S}}(\pi_{\theta})$ respectively. To handle the generalization loss, we develop the following theorem.

Theorem 3.3 (Generalization via local robustness). *Denote $L = (1 + \epsilon_h)G^{1/2}$. Under assumption $\mathcal{L}_{\mathcal{D}}(\theta) \leq E_{\epsilon_i \sim N(0, \rho)} \mathcal{L}_{\mathcal{D}}(\theta + \epsilon)$ similar to SAM (Foret et al., 2021), with probability at least $1 - \delta$ over $\mathcal{S} \sim \mathcal{D}^N$, we have*

$$\begin{aligned} \mathcal{L}_{\mathcal{D}}(\pi_{\theta}) &\leq \max_{\|\theta' - \theta\| \leq \rho} \mathcal{L}_{\mathcal{S}}(\pi_{\theta'}) + \frac{8L}{\sqrt{N}} \sqrt{\log \frac{N+d}{\delta}} \\ &+ \frac{4L}{\sqrt{N}} O(1) + \frac{4L}{\sqrt{N}} d \log \left(1 + \frac{\|\theta\|_2^2}{\rho} \left(1 + \sqrt{\frac{\log N}{d}} \right) \right), \end{aligned} \quad (14)$$

where $d = |\theta|$ is the model size and $\rho > 0$ is the perturbation radius.

Our proof is adopted from SAM (Foret et al., 2021), but our result is more general because it is applicable to any bounded loss function, thanks to the general PAC-Bayes theorem (Alquier et al., 2016) we apply. Moreover, a first-order expansion around θ yields the approximation

$$\max_{\|\theta' - \theta\| \leq \rho} \mathcal{L}_{\mathcal{S}}(\pi_{\theta'}) \approx \mathcal{L}_{\mathcal{S}}(\pi_{\theta}) + \rho \|\nabla_{\theta} \mathcal{L}_{\mathcal{S}}(\pi_{\theta})\|_2, \quad (15)$$

which highlights two complementary targets for better generalization: (i) reducing the empirical loss, and (ii) reducing the *sharpness* term measured by the gradient norm. This section develops a token-level view of how GRPO shapes $\|\nabla_{\theta} \mathcal{L}_{\mathcal{S}}(\pi_{\theta})\|_2$, and proposes a probability-aware reweighting that directly suppresses sharp directions while preserving learning signal on semantically critical tokens.

3.2. Sharpness-Guided GRPO for better generalization

Motivated by Eq. (14)-(15), we aim to reduce sharpness by explicitly controlling token-level gradient magnitudes. Following the generalization development, we introduce an increasing *probability shaping* function $\omega(\cdot)$ and define a token weight $w_{i,t} := \omega(\pi_{\theta}(o_{i,t}))$. This yields a weighted GRPO surrogate that remains compatible with PPO/GRPO clipping and advantage learning, while steering optimization toward flatter (less sharp) regions.

We rewrite the empirical loss of (13):

$$\begin{aligned} \mathcal{L}_{\mathcal{S}}(\pi_{\theta}) &= \mathbb{E}_{(q, o_{1:G}) \sim \mathcal{S}} \left[\frac{1}{\sum_{i=1}^G |o_i|} \sum_{i=1}^G \sum_{t=1}^{|o_i|} \min\{w_{i,t} \times \right. \\ &\quad \left. r_{i,t}(\theta) \hat{A}_{i,t}, \text{clip}(w_{i,t} r_{i,t}(\theta), 1 - \epsilon_l, 1 + \epsilon_h) \hat{A}_{i,t}\} \right. \\ &\quad \left. - \beta \mathbb{D}_{\text{KL}}[\pi_{\theta} \parallel \pi_{\text{ref}}] \right]. \end{aligned}$$

$$\text{where } r_{i,t}(\theta) \triangleq \frac{\pi_{\theta}(o_{i,t} | q, o_{i,<t})}{\pi_{\theta_{\text{old}}}(o_{i,t} | q, o_{i,<t})}.$$

We now investigate the gradient of the empirical loss $\mathcal{L}_{\mathcal{S}}(\pi_{\theta})$.

Lemma 3.4. *We have the following*

$$\begin{aligned} &\nabla_{\theta} \mathcal{L}_{\mathcal{S}}(\pi_{\theta}) \\ &= \mathbb{E}_{(q, \{o_i\}_{i=1}^G) \sim \mathcal{S}} \left[\frac{1}{\sum_{i=1}^G |o_i|} \sum_{i=1}^G \sum_{t=1}^{|o_i|} w_{i,t} \nabla_{\theta} \log \pi_{\theta}(o_{i,t}) \times \right. \\ &\quad \left. \underbrace{\left(\frac{\pi_{\theta}(o_{i,t})}{\pi_{\text{old}}(o_{i,t})} \hat{A}_{i,t} \cdot \mathbb{I}_{\text{trust}} \left(\frac{\pi_{\theta}(o_{i,t})}{\pi_{\text{old}}(o_{i,t})}, \hat{A}_{i,t} \right) + \beta \frac{\pi_{\text{ref}}(o_{i,t})}{\pi_{\theta}(o_{i,t})} - \beta \right)}_{\gamma_{i,t}} \right], \end{aligned}$$

where we have defined $\mathbb{I}_{\text{trust}} \left(\frac{\pi_{\theta}(o_{i,t})}{\pi_{\text{old}}(o_{i,t})}, \hat{A}_{i,t} \right)$ as

$$\mathbb{I}_{\text{trust}} = \begin{cases} 0, & \text{if } \hat{A}_{i,t} > 0 \text{ and } \frac{\pi_{\theta}(o_{i,t})}{\pi_{\text{old}}(o_{i,t})} > w_{i,t}^{-1} (1 + \epsilon_h), \\ 0, & \text{if } \hat{A}_{i,t} < 0 \text{ and } \frac{\pi_{\theta}(o_{i,t})}{\pi_{\text{old}}(o_{i,t})} < w_{i,t}^{-1} (1 - \epsilon_l), \\ 1, & \text{otherwise.} \end{cases}$$

We represent our LLM as the composition of many layers $f = f_L \circ f_{L-1} \circ \dots \circ f_l \circ \dots \circ f_1$ where f maps from the input sequence of tokens a_0 to the output sequence of tokens a_L . Moreover, the output sequence of tokens a_L is used to compute the logit $h_{i,t}$ for predicting the token $o_{i,t}$. Let us denote a_{l-1} and a_l as the input and output of the l -th layer, i.e., $a_l = f_l(a_{l-1}, \theta_l)$ where θ_l represents the model parameter at the l -th layer. To quantify the gradient for update, we develop the following theorem.

Theorem 3.5. *Let us denote the classifier head at the output layer, the Jacobian $\frac{\partial f_l(a_{l-1}, \theta_l)}{\partial a_{l-1}}$, and the gradient matrix $\frac{\partial f_l(a_{l-1}, \theta_l)}{\partial \theta_l}$ as W, J_l , and G_l respectively. Moreover, we further assume that $\sigma_{\min}(W) \geq (\alpha^W)^2$, $\sigma_{\max}(W) \leq (\beta^W)^2$, $\sigma_{\min}(J_l) \geq (\alpha_l^J)^2$, $\sigma_{\max}(J_l) \leq (\beta_l^J)^2$, and $\sigma_{\min}(G_l) \geq (\alpha_l^G)^2$, $\sigma_{\max}(G_l) \leq (\beta_l^G)^2$ where all lower/upper bounds are positive and $\sigma_{\min}(\cdot)$, $\sigma_{\max}(\cdot)$ return the smallest and the largest singular values of a matrix. We can bound the gradient norm $\|g_{i,t}\|_2$ where $g_{i,t} = \gamma_{i,t} w_{i,t} \nabla_{\theta} \log \pi_{\theta}(o_{i,t})$:*

$$\frac{w_{i,t}(1 - \pi_{\theta}(o_{i,t}))}{\sqrt{L}} L_{i,t} \leq \|g_{i,t}\|_2 \leq \sqrt{2} w_{i,t} (1 - \pi_{\theta}(o_{i,t})) U_{i,t}, \quad (16)$$

where we have defined

$$\begin{aligned} L_{i,t} &= |\gamma_{i,t}| \sum_{l=1}^L \left(a_l^W a_l^G \prod_{j=l}^L a_j^J \right), \\ U_{i,t} &= |\gamma_{i,t}| \sum_{l=1}^L \left(b_l^W b_l^G \prod_{j=l}^L b_j^J \right). \end{aligned}$$

With the support of the bounds in Theorem 3.5, we develop the lower and upper bounds for $\|\nabla_{\theta} \mathcal{L}_{\mathcal{S}}(\pi_{\theta})\|_2$.

Theorem 3.6. Let $d = |\theta|$ be the model size. We have

(i) The upper bound of $\|\nabla_{\theta} \mathcal{L}_{\mathcal{S}}(\pi_{\theta})\|_2$ is

$$\|\nabla_{\theta} \mathcal{L}_{\mathcal{S}}(\pi_{\theta})\|_2 \leq \mathbb{E}_{\mathcal{S}} \left[\frac{\sqrt{2}}{\sum_i^G |o_i|} \sum_{i=1}^G \sum_{t=1}^{|o_i|} w_{i,t} (1 - \pi(o_{i,t})) U_{i,t} \right] \quad (17)$$

(ii) For any $\delta \in (0, 1)$, with probability at least $1 - \delta$, we have

$$\begin{aligned} \|\nabla_{\theta} \mathcal{L}_{\mathcal{S}}(\pi_{\theta})\|_2 \geq & \left[\frac{1}{|\mathcal{S}|^2} \mathbb{E}_{\mathcal{S}} \left[\left(\sum_{i=1}^G \sum_{t=1}^{|o_i|} \frac{w_{i,t} (1 - \pi_{\theta}(o_{i,t})) L_{i,t}}{(\sum_{i=1}^G |o_i|)^{3/2} \sqrt{L}} \right)^2 \right] \right. \\ & \left. - 2\epsilon \mathbb{E}_{\mathcal{S} \times \mathcal{S}} \left[\left(\sum_{i=1}^G \sum_{t=1}^{|o_i|} \frac{w_{i,t} (1 - \pi_{\theta}(o_{i,t})) U_{i,t}}{\sum_i |o_i|} \right) \times \right. \right. \\ & \left. \left. \left(\sum_{i=1}^G \sum_{t=1}^{|o'_i|} \frac{w'_{i,t} (1 - \pi_{\theta}(o'_{i,t})) U'_{i,t}}{\sum_{i'} |o'_i|} \right) \right] \right]^{1/2} \quad (18) \end{aligned}$$

where we define $\epsilon = \sqrt{\frac{1}{cd} (\log(CK^2) + \log \frac{1}{\delta})}$ with two positive constants c, C and $K = \sum_{k=1}^N \sum_{i=1}^G |o_{ki}|$.

It is worth noting that, because the model size $d = |\theta|$ is usually very high for LLMs, the second term $2\epsilon \mathbb{E}_{\mathcal{S} \times \mathcal{S}}[\dots]$ is usually negligible, and the lower bound of $\|\nabla_{\theta} \mathcal{L}_{\mathcal{S}}(\pi_{\theta})\|_2$ is dominated by the first term.

According to the upper bound in (17) and the lower bound in (18), we need to set the weights $w_{i,t}$ to minimize $w_{i,t} (1 - \pi(o_{i,t}))$, reduce the gradient norm $\|\nabla_{\theta} \mathcal{L}_{\mathcal{S}}(\pi_{\theta})\|_2$, and stabilize the gradients.

We hence instantiate $w_{i,t}$ with a monotone, probability-aware mapping and stop-gradient to avoid the model gaming the weights. Inspired by recent advances in token-level preference optimization (Liu et al., 2024; Le et al., 2025), we instantiate $w_{i,t}$ as:

$$w_{i,t} = \text{clip} \left(\alpha \cdot \left[\sigma \left(\frac{\text{sg}[\pi_{\theta}(o_{i,t} | q, o_{i,t} < t)]}{\tau} \right) - \mu \right], L, U \right), \quad (19)$$

where $\text{sg}[\cdot]$ is the stop-gradient operator.

For low-probability tokens, $(1 - \pi_{\theta}(o_{i,t}))$ is large while $w_{i,t}$ is small; for high-probability tokens, $(1 - \pi_{\theta}(o_{i,t}))$ is small while $w_{i,t}$ is large. Thus, GRPO-SG stabilizes the product $w_{i,t} (1 - \pi_{\theta}(o_{i,t}))$ across tokens, suppressing extreme token gradients that would otherwise dominate $\|\nabla_{\theta} \mathcal{L}_{\mathcal{S}}(\pi_{\theta})\|_2$. By Eq. (15), reducing this gradient norm directly reduces sharpness, which tightens the robust empirical bound in Eq. (14) and improves generalization.

Eq. (15) suggests that smaller gradient norms correspond to less sharp updates and hence better generalization. From Theorems 3.6 and 3.5, GRPO-SG suppresses extreme token

gradients through the stabilizing factor $w_{i,t} (1 - \pi_{\theta}(o_{i,t}))$. To validate this mechanism, we track gradient norms during training under three RLVR settings in Figure 1. Compared to GRPO, GRPO-SG exhibits smaller fluctuations and fewer outlier spikes, consistent with reduced sharpness and improved generalization.

In addition to gradient-norm analysis, we also track training rewards across math reasoning, agentic and logic settings in Figure 2. GRPO-SG yields higher and more stable reward trajectories than GRPO, indicating more effective learning while simultaneously controlling sharpness.

4. Experiments

We conduct extensive experiments across multiple RLVR benchmarks to assess the effectiveness of GRPO-SG. The results demonstrate that our method consistently outperforms GRPO, delivering stronger reasoning ability and more stable training dynamics.

4.1. Experimental Setup

To validate the effectiveness and generality of our proposed method, we conduct experiments in three widely used RLVR settings that stress different aspects of reasoning: (i) Math reasoning, (ii) Agentic and (iii) Logic.

For **mathematical** reasoning tasks, where correctness can be verified automatically against gold-standard answers. Following (Yang et al., 2025c), we train on datasets that combine symbolic manipulation and arithmetic word problems, using a binary reward signal: 1 if the final boxed answer matches the reference solution and 0 otherwise. The training corpus includes diverse math reasoning prompts designed to encourage structured derivations rather than direct guessing. For evaluation, we adopt multiple benchmarks that are standard in math-focused RLVR research: Olympiad Bench (Hendrycks et al., 2021), Minerva (Lewkowycz et al., 2022), MATH-500 (He et al., 2024), AMC 2022-2023 and AIME 2024. For the first three benchmarks, evaluation is conducted using greedy decoding. For the last two benchmarks, consistent with standard practice, we generate 16 responses per question and report the mean accuracy across these samples (avg@16). Notably, since AIME 2024 is an extremely challenging dataset, we also report pass@16, which counts a problem as solved if at least one of the 16 responses is correct.

We next consider **agentic** reasoning tasks, we examine an agentic setting that requires knowledge-intensive reasoning augmented with retrieval tools. Following the **Search-R1** (Jin et al., 2025) configuration from **VeriTool** framework (Jiang et al., 2025), the model interacts with an external tool server providing a retriever and other utilities such as Python or SQL. Training data consists of open-domain

Table 1. Experimental results on math-related datasets (DSR for DeepScaleR and ORZ for Open Reasoner-Zero). The best results are indicated in **bold**.

Dataset	Algorithms	Olympiad Bench	Minerva	MATH 500	AMC avg@16	AIME pass@16	AIME avg@16	Avg.
	Qwen2.5-7B	27.64	18.38	63.00	22.21	30.00	5.00	27.71
DSR	+ GRPO	36.50	29.66	74.67	47.72	28.89	16.46	38.98
	+ GRPO-SG	38.48	32.35	79.40	46.84	43.33	18.13	43.09 $\uparrow 10.5\%$
ORZ	+ GRPO	38.23	27.69	78.33	49.57	32.22	12.92	39.83
	+ GRPO-SG	40.12	30.51	78.60	45.48	43.33	16.88	42.49 $\uparrow 6.7\%$

QA datasets where each instance requires grounding reasoning steps with retrieved evidence. The reward is based on exact-match correctness of the final answer, while intermediate tool calls are masked in the policy loss to avoid leakage of supervision. For evaluation, we follow the VerlTool benchmark and report exact-match accuracy on both General Q&A benchmarks (NQ (Kwiatkowski et al., 2019), TriviaQA (Joshi et al., 2017), PopQA (Mallen et al., 2022)) and multi-hop Q&A benchmark (HotpotQA (Yang et al., 2018), 2Wiki (Ho et al., 2020), MuSiQue (Trivedi et al., 2022), Bamboogle (Press et al., 2022)).

For the **logic** data, following (Yang et al., 2025c), we adopt the K&K (Knights and Knaves) logic puzzles introduced in (Xie et al., 2024). Each puzzle describes a set of people who always lie or always tell the truth, and the task is to determine their identities given a set of statements. For training, we use the same dataset splits as in (Yang et al., 2025c), which include synthetic instances of increasing difficulty from 3 to 7 (measured by the number of people per puzzle). The reward function checks both the output format (requiring explicit <think> and <answer> tags) and the correctness of the final assignment. During evaluation, we follow the official harness and report accuracy across all difficulty levels, as well as breakdowns by puzzle size. This setting emphasizes step-by-step deductive reasoning and tests whether the model can align reasoning traces with verifiable logical consistency.

We leave further implementation details and hyperparameters to Appendix B with detailed evaluation setting adopted by our experiments.

4.2. Main Results

Besides the detailed analysis of low and high-probability tokens in Section 3, we now present the main empirical results of our study. Across all three widely used RLVR settings include math, agentic and logic our proposed GRPO-SG method achieves substantial and consistent gains over the widely used GRPO baseline.

4.2.1. EXPERIMENTS ON MATH-RELATED DATASETS

To further demonstrate the effectiveness of our method, we conducted experiments on Math-related datasets. Table 1 summarizes performance on mathematical reasoning datasets. GRPO-SG consistently surpasses GRPO, with average gains of 6–10% across OlympiadBench, Minerva, MATH-500, AMC, and AIME. In particular, on AIME, GRPO-SG raises pass@16 from 16.5% to 18.1% and average@16 from 28.9% to 43.3%, demonstrating stronger robustness in symbolic and arithmetic reasoning. These results clearly highlight the superiority of our proposed GRPO-SG over GRPO baseline in advancing mathematical reasoning.

4.2.2. EXPERIMENTS ON AGENTIC VERLTOOL SEARCH

To extend our evaluation, we further examine GRPO-SG on agentic RLVR tasks. Table 2 presents results in the agentic RLVR setting, where GRPO-SG delivers the largest improvements. On knowledge-intensive QA tasks, GRPO-SG nearly doubles the performance of GRPO, improving average exact-match accuracy from 13.8 to 27.3 ($\uparrow 97\%$) for Qwen2.5-3B, and yielding a 14% relative gain on Qwen3-4B-Instruct-2507. These results confirm the effectiveness of token-level regulation in tool-augmented reasoning, where stability and precision are critical. Together, these results establish GRPO-SG as a consistently stronger optimization method than GRPO across diverse RLVR domains, with particularly striking gains in logic puzzles and agentic reasoning.

4.2.3. EXPERIMENTS ON K&K LOGIC PUZZLES

Table 3 reports results on the K&K Logic Puzzles benchmark, where GRPO-SG achieves significant improvements over GRPO across all difficulty levels. Notably, GRPO-SG boosts the average accuracy of Qwen2.5-3B from 39% (with GRPO) to 63%, representing a relative gain of over 60%. Similarly, for Qwen2.5-7B, GRPO-SG increases the average accuracy from 77% to 91% (+18%). It is worth noting that this task remains challenging even for powerful proprietary models such as GPT-4o, DeepSeek-R1, and o1,

Table 2. Experimental results for the agentic task using VT-Search on knowledge-QA benchmarks. † represents in-domain datasets and * represents out-domain datasets. The best results are indicated in **bold**.

Model	General QA			Multi-hop QA				Avg.
	NQ	TriviaQA	PopQA	HQA	2Wiki	Musique	Bamboogle	
Qwen2.5-3B	0.50	1.20	0.80	0.50	1.50	0.00	0.00	0.64
+ GRPO	13.50	29.40	11.50	14.50	16.30	1.30	10.40	13.84
+ GRPO-SG	41.80	52.30	39.10	24.50	20.30	5.00	8.00	27.29 †97.2%
Qwen3-4B	31.68	60.00	38.60	27.59	14.89	6.70	23.20	28.95
+ GRPO	46.48	59.84	40.39	35.54	28.87	10.26	27.20	35.21
+ GRPO-SG	48.23	64.11	46.00	36.60	30.89	10.26	41.60	40.18 †14.1%

Table 3. Experimental results on the K&K Logic Puzzles benchmark. The best results are indicated in **bold**.

Model	Difficulty by Number of People					Avg.
	3	4	5	6	7	
GPT-4o	0.57	0.49	0.32	0.23	0.21	0.36
o1-2024-12-17	0.51	0.38	0.38	0.35	0.30	0.38
Deepseek-R1	0.73	0.77	0.78	0.75	0.88	0.78
Qwen2.5-3B-Instruct	0.09	0.10	0.03	0.05	0.02	0.06
+ GRPO	0.64	0.47	0.35	0.30	0.21	0.39
+ GRPO-SG	0.76	0.76	0.61	0.59	0.44	0.63 †61.5%
Qwen2.5-7B-Instruct-1M	0.22	0.15	0.08	0.10	0.02	0.11
+ GRPO	0.91	0.91	0.77	0.65	0.61	0.77
+ GRPO-SG	0.95	0.95	0.92	0.87	0.84	0.91 †18.2%

Table 4. Computational cost comparison of GRPO and GRPO-SG on K&K Logic Puzzle Dataset. Training time is reported in minutes per sample; peak GPU memory is reported in GB.

	Qwen2.5-3B		LLaMa3.1-8B	
	GRPO	GRPO-SG	GRPO	GRPO-SG
Training Time/Sample	271.4	286.0	678.5	722.2
Peak Mem	459.7	460.2	581.2	580.6

which achieve average accuracies of only 36–78%.

4.3. Computational Costs

Table 4 reports the computational overhead of applying GRPO-SG compared to the GRPO baseline on the K&K Logic Puzzles dataset. The only additional operation required by GRPO-SG is the computation of token-level weights. Importantly, these weights are derived directly from the model’s own output probabilities and therefore do not require any auxiliary extra forward passes. As a result, peak GPU memory usage remains essentially unchanged between GRPO and GRPO-SG across both the Qwen2.5-3B-Instruct and LLaMa3.1-8B-Instruct backbones.

In terms of runtime, GRPO-SG does introduce a modest

increase in training time per sample (e.g., 271.4 vs. 286.0 minutes on Qwen2.5-3B-Instruct, and 678.5 vs. 722.2 minutes on LLaMa3.1-8B-Instruct). However, this overhead is relatively minor compared to the substantial performance improvements reported in Section 4. Together, these results confirm that GRPO-SG delivers consistent gains in reasoning performance without imposing significant additional computational costs.

5. Conclusion

In this work, we revisit GRPO for RLVR from a generalization perspective and introduce GRPO-SG, a sharpness-guided variant of GRPO that uses the model confidence to shape updates and reduce overly sharp gradient steps during RLVR training. Our analysis connects update sharpness to probability-dependent terms in gradient norms, motivating a simple modification to the GRPO objective. Across diverse settings, GRPO-SG delivers consistent improvements over GRPO. Overall, the results suggest that explicitly controlling update sharpness is an effective way to improve the stability and performance of RL-trained models.

Limitations. A key limitation of GRPO-SG is the extra compute from token-level weighting. Each update estimates and applies weights to all generated tokens, slightly increasing per-step cost over standard GRPO. However, as shown in Section 4.3, the overhead is acceptable in practice and does not limit scalability to larger models or datasets.

Impact Statement

This paper proposes GRPO-SG, a probability-shaped token-weighting extension of GRPO that aims to improve generalization and training stability in reinforcement learning with verifiable rewards for language model reasoning. Potential positive societal impacts include more reliable and robust language models for many applications such as education, decision support, and retrieval-augmented question answering. We do not feel there are specific negative ethical consequences that must be highlighted here.

References

- Abbas, M., Xiao, Q., Chen, L., Chen, P.-Y., and Chen, T. Sharp-maml: Sharpness-aware model-agnostic meta learning. *arXiv preprint arXiv:2206.03996*, 2022.
- Alquier, P., Ridgway, J., and Chopin, N. On the properties of variational approximations of gibbs posteriors. *Journal of Machine Learning Research*, 17(236), 2016. URL <http://jmlr.org/papers/v17/15-290.html>.
- Bahri, D., Mobahi, H., and Tay, Y. Sharpness-aware minimization improves language model generalization. In *Proceedings of the 60th Annual Meeting of the Association for Computational Linguistics (Volume 1: Long Papers)*, pp. 7360–7371, Dublin, Ireland, May 2022. Association for Computational Linguistics. doi: 10.18653/v1/2022.acl-long.508. URL <https://aclanthology.org/2022.acl-long.508>.
- Cha, J., Chun, S., Lee, K., Cho, H.-C., Park, S., Lee, Y., and Park, S. Swad: Domain generalization by seeking flat minima. *Advances in Neural Information Processing Systems*, 34:22405–22418, 2021.
- Chandra, A., Agrawal, A., Hosseini, A., Fischmeister, S., Agarwal, R., Goyal, N., and Courville, A. Shape of thought: When distribution matters more than correctness in reasoning tasks. *arXiv preprint arXiv:2512.22255*, 2025. URL <https://arxiv.org/abs/2512.22255>.
- Chen, X., Hsieh, C.-J., and Gong, B. When vision transformers outperform resnets without pre-training or strong data augmentations. *arXiv preprint arXiv:2106.01548*, 2021.
- Cobbe, K., Kosaraju, V., Bavarian, M., Chen, M., Jun, H., Kaiser, L., Plappert, M., Tworek, J., Hilton, J., Nakano, R., et al. Training verifiers to solve math word problems. *arXiv preprint arXiv:2110.14168*, 2021.
- Deng, J., Pang, J., Zhang, B., and Guo, G. Asymptotic unbiased sample sampling to speed up sharpness-aware minimization. In *Proceedings of the AAAI Conference on Artificial Intelligence*, volume 39, pp. 16208–16216, 2025.
- Dziugaite, G. K. and Roy, D. M. Computing nonvacuous generalization bounds for deep (stochastic) neural networks with many more parameters than training data. In *UAI*. AUAI Press, 2017.
- Ethayarajh, K., Xu, W., Muennighoff, N., Jurafsky, D., and Kiela, D. Kto: Model alignment as prospect theoretic optimization. *arXiv preprint arXiv:2402.01306*, 2024.
- Foret, P., Kleiner, A., Mobahi, H., and Neyshabur, B. Sharpness-aware minimization for efficiently improving generalization. In *International Conference on Learning Representations*, 2021. URL <https://openreview.net/forum?id=6Tm1mposlrM>.
- Gao, J., Xu, S., Ye, W., Liu, W., He, C., Fu, W., Mei, Z., Wang, G., and Wu, Y. On designing effective rl reward at training time for llm reasoning. *arXiv preprint arXiv:2410.15115*, 2024.
- Guan, X., Zhang, L. L., Liu, Y., Shang, N., Sun, Y., Zhu, Y., Yang, F., and Yang, M. rstar-math: Small llms can master math reasoning with self-evolved deep thinking. *arXiv preprint arXiv:2501.04519*, 2025.
- Guo, D., Yang, D., Zhang, H., Song, J., Zhang, R., Xu, R., Zhu, Q., Ma, S., Wang, P., Bi, X., et al. Deepseek-r1: Incentivizing reasoning capability in llms via reinforcement learning. *arXiv preprint arXiv:2501.12948*, 2025.
- He, C., Luo, R., Bai, Y., Hu, S., Thai, Z. L., Shen, J., Hu, J., Han, X., Huang, Y., Zhang, Y., et al. Olympiadbench: A challenging benchmark for promoting agi with olympiad-level bilingual multimodal scientific problems. *arXiv preprint arXiv:2402.14008*, 2024.
- Hendrycks, D., Burns, C., Kadavath, S., Arora, A., Basart, S., Tang, E., Song, D., and Steinhardt, J. Measuring mathematical problem solving with the math dataset. *arXiv preprint arXiv:2103.03874*, 2021.
- Hendrycks, D., Burns, C., Kadavath, S., Arora, A., Basart, S., Tang, E., Song, D., and Steinhardt, J. Measuring mathematical problem solving with the math dataset, 2021. URL <https://arxiv.org/abs/2103.03874>, 2, 2024.
- Ho, X., Nguyen, A.-K. D., Sugawara, S., and Aizawa, A. Constructing a multi-hop qa dataset for comprehensive evaluation of reasoning steps. *arXiv preprint arXiv:2011.01060*, 2020.
- Hu, J., Zhang, Y., Han, Q., Jiang, D., Zhang, X., and Shum, H.-Y. Open-reasoner-zero: An open source approach to scaling up reinforcement learning on the base model. *arXiv preprint arXiv:2503.24290*, 2025.
- Hu, Y., Wang, W., Jia, H., Wang, Y., Chen, Y., Hao, J., Wu, F., and Fan, C. Learning to utilize shaping rewards: A new approach of reward shaping. *Advances in Neural Information Processing Systems*, 33:15931–15941, 2020.
- Huang, B., Xie, Y., and Xu, C. Learning with noisy labels via clean aware sharpness aware minimization. *Scientific Reports*, 15(1):1350, 2025.
- Jaech, A., Kalai, A., Lerer, A., Richardson, A., El-Kishky, A., Low, A., Helyar, A., Madry, A., Beutel, A., Carney, A., et al. Openai o1 system card. *arXiv preprint arXiv:2412.16720*, 2024.

- Jain, N., Han, K., Gu, A., Li, W.-D., Yan, F., Zhang, T., Wang, S., Solar-Lezama, A., Sen, K., and Stoica, I. Livecodebench: Holistic and contamination free evaluation of large language models for code. *arXiv preprint arXiv:2403.07974*, 2024.
- Jastrzebski, S., Kenton, Z., Arpit, D., Ballas, N., Fischer, A., Bengio, Y., and Storkey, A. J. Three factors influencing minima in sgd. *ArXiv*, abs/1711.04623, 2017.
- Jiang, D., Lu, Y., Li, Z., Lyu, Z., Nie, P., Wang, H., Su, A., Chen, H., Zou, K., Du, C., et al. Verltool: Towards holistic agentic reinforcement learning with tool use. *arXiv preprint arXiv:2509.01055*, 2025.
- Jiang, Y., Neyshabur, B., Mobahi, H., Krishnan, D., and Bengio, S. Fantastic generalization measures and where to find them. In *ICLR*. OpenReview.net, 2020.
- Jin, B., Zeng, H., Yue, Z., Yoon, J., Arik, S., Wang, D., Zamani, H., and Han, J. Search-rl: Training llms to reason and leverage search engines with reinforcement learning. *arXiv preprint arXiv:2503.09516*, 2025.
- Joshi, M., Choi, E., Weld, D. S., and Zettlemoyer, L. Triviaqa: A large scale distantly supervised challenge dataset for reading comprehension. *arXiv preprint arXiv:1705.03551*, 2017.
- Karpukhin, V., Oguz, B., Min, S., Lewis, P. S., Wu, L., Edunov, S., Chen, D., and Yih, W.-t. Dense passage retrieval for open-domain question answering. In *EMNLP (1)*, pp. 6769–6781, 2020.
- Keskar, N. S., Mudigere, D., Nocedal, J., Smelyanskiy, M., and Tang, P. T. P. On large-batch training for deep learning: Generalization gap and sharp minima. In *ICLR*. OpenReview.net, 2017.
- Kwiatkowski, T., Palomaki, J., Redfield, O., Collins, M., Parikh, A., Alberti, C., Epstein, D., Polosukhin, I., Devlin, J., Lee, K., et al. Natural questions: a benchmark for question answering research. *Transactions of the Association for Computational Linguistics*, 7:453–466, 2019.
- Kwon, J., Kim, J., Park, H., and Choi, I. K. Asam: Adaptive sharpness-aware minimization for scale-invariant learning of deep neural networks. In *International Conference on Machine Learning*, pp. 5905–5914. PMLR, 2021.
- Lambert, N., Morrison, J., Pyatkin, V., Huang, S., Ivison, H., Brahman, F., Miranda, L. J. V., Liu, A., Dziri, N., Lyu, S., et al. Tulu 3: Pushing frontiers in open language model post-training. *arXiv preprint arXiv:2411.15124*, 2024.
- Le, T., Vuong, H. T., Tran, Q., Van, L. N., Harandi, M., and Le, T. Token-level self-play with importance-aware guidance for large language models. In *The Thirty-ninth Annual Conference on Neural Information Processing Systems*, 2025.
- Lewkowycz, A., Andreassen, A., Dohan, D., Dyer, E., Michalewski, H., Ramasesh, V., Slone, A., Anil, C., Schlag, I., Gutman-Solo, T., et al. Solving quantitative reasoning problems with language models. *Advances in neural information processing systems*, 35:3843–3857, 2022.
- Liu, A., Bai, H., Lu, Z., Sun, Y., Kong, X., Wang, S., Shan, J., Jose, A. M., Liu, X., Wen, L., et al. Tisdpo: Token-level importance sampling for direct preference optimization with estimated weights. *arXiv preprint arXiv:2410.04350*, 2024.
- Liu, J., Liu, G., Liang, J., Li, Y., Liu, J., Wang, X., Wan, P., Zhang, D., and Ouyang, W. Flow-grpo: Training flow matching models via online rl. *arXiv preprint arXiv:2505.05470*, 2025.
- Liu, S.-Y., Dong, X., Lu, X., Diao, S., Belcak, P., Liu, M., Chen, M.-H., Yin, H., Wang, Y.-C. F., Cheng, K.-T., Choi, Y., Kautz, J., and Molchanov, P. Gdpo: Group reward-decoupled normalization policy optimization for multi-reward rl optimization, 2026. URL <https://arxiv.org/abs/2601.05242>.
- Ma, X., Liu, Q., Jiang, D., Zhang, G., Ma, Z., and Chen, W. General-reasoner: Advancing llm reasoning across all domains. *arXiv preprint arXiv:2505.14652*, 2025.
- Mallen, A., Asai, A., Zhong, V., Das, R., Khashabi, D., and Hajishirzi, H. When not to trust language models: Investigating effectiveness of parametric and non-parametric memories. *arXiv preprint arXiv:2212.10511*, 2022.
- Meng, Y., Xia, M., and Chen, D. Simpo: Simple preference optimization with a reference-free reward. *Advances in Neural Information Processing Systems*, 37:124198–124235, 2024.
- Nguyen, V.-A., Vuong, T.-L., Phan, H., Do, T.-T., Phung, D., and Le, T. Flat seeking bayesian neural network. In *Advances in Neural Information Processing Systems*, 2023.
- Ouyang, L., Wu, J., Jiang, X., Almeida, D., Wainwright, C., Mishkin, P., Zhang, C., Agarwal, S., Slama, K., Ray, A., et al. Training language models to follow instructions with human feedback. *Advances in neural information processing systems*, 35:27730–27744, 2022.
- Pan, J., Liu, C., Wu, J., Liu, F., Zhu, J., Li, H. B., Chen, C., Ouyang, C., and Rueckert, D. Medvlm-rl: Incentivizing medical reasoning capability of vision-language models (vlms) via reinforcement learning. In *International*

- Conference on Medical Image Computing and Computer-Assisted Intervention*, pp. 337–347. Springer, 2025.
- Petzka, H., Kamp, M., Adilova, L., Sminchisescu, C., and Boley, M. Relative flatness and generalization. In *NeurIPS*, pp. 18420–18432, 2021.
- Phan, H., Tran, N., Le, T., Tran, T., Ho, N., and Phung, D. Stochastic multiple target sampling gradient descent. *Advances in neural information processing systems*, 2022.
- Press, O., Zhang, M., Min, S., Schmidt, L., Smith, N. A., and Lewis, M. Measuring and narrowing the compositionality gap in language models. *arXiv preprint arXiv:2210.03350*, 2022.
- Qu, Z., Li, X., Duan, R., Liu, Y., Tang, B., and Lu, Z. Generalized federated learning via sharpness aware minimization. *arXiv preprint arXiv:2206.02618*, 2022.
- Rafailov, R., Sharma, A., Mitchell, E., Manning, C. D., Ermon, S., and Finn, C. Direct preference optimization: Your language model is secretly a reward model. *Advances in neural information processing systems*, 36: 53728–53741, 2023.
- Rein, D., Hou, B. L., Stickland, A. C., Petty, J., Pang, R. Y., Dirani, J., Michael, J., and Bowman, S. R. Gpqa: A graduate-level google-proof q&a benchmark. In *First Conference on Language Modeling*, 2024.
- Schulman, J., Wolski, F., Dhariwal, P., Radford, A., and Klimov, O. Proximal policy optimization algorithms. *arXiv preprint arXiv:1707.06347*, 2017.
- Shao, Z., Wang, P., Zhu, Q., Xu, R., Song, J., Bi, X., Zhang, H., Zhang, M., Li, Y., Wu, Y., et al. Deepseekmath: Pushing the limits of mathematical reasoning in open language models. *arXiv preprint arXiv:2402.03300*, 2024.
- Song, H., Jiang, J., Min, Y., Chen, J., Chen, Z., Zhao, W. X., Fang, L., and Wen, J.-R. R1-searcher: Incentivizing the search capability in llms via reinforcement learning. *arXiv preprint arXiv:2503.05592*, 2025.
- Tan, C., Zhang, J., Liu, J., Wang, Y., and Hao, Y. Stabilizing sharpness-aware minimization through a simple renormalization strategy. *Journal of Machine Learning Research*, 26(68):1–35, 2025.
- Tang, Y., Guo, D. Z., Zheng, Z., Calandriello, D., Cao, Y., Tarassov, E., Munos, R., Pires, B. Á., Valko, M., Cheng, Y., et al. Understanding the performance gap between online and offline alignment algorithms. *arXiv preprint arXiv:2405.08448*, 2024.
- Team, K., Du, A., Gao, B., Xing, B., Jiang, C., Chen, C., Li, C., Xiao, C., Du, C., Liao, C., et al. Kimi k1. 5: Scaling reinforcement learning with llms. *arXiv preprint arXiv:2501.12599*, 2025.
- Trivedi, H., Balasubramanian, N., Khot, T., and Sabharwal, A. MuSiQue: Multihop questions via single-hop question composition. *Transactions of the Association for Computational Linguistics*, 2022.
- Vaswani, A., Shazeer, N., Parmar, N., Uszkoreit, J., Jones, L., Gomez, A. N., Kaiser, Ł., and Polosukhin, I. Attention is all you need. *Advances in neural information processing systems*, 30, 2017.
- Wang, L., Yang, N., Huang, X., Jiao, B., Yang, L., Jiang, D., Majumder, R., and Wei, F. Text embeddings by weakly-supervised contrastive pre-training. *arXiv preprint arXiv:2212.03533*, 2022.
- Wang, X., Li, B., Song, Y., Xu, F. F., Tang, X., Zhuge, M., Pan, J., Song, Y., Li, B., Singh, J., et al. Openhands: An open platform for ai software developers as generalist agents. *arXiv preprint arXiv:2407.16741*, 2024.
- Wang, Y., Yang, Q., Zeng, Z., Ren, L., Liu, L., Peng, B., Cheng, H., He, X., Wang, K., Gao, J., et al. Reinforcement learning for reasoning in large language models with one training example. *arXiv preprint arXiv:2504.20571*, 2025.
- Wei, C., Kakade, S., and Ma, T. The implicit and explicit regularization effects of dropout. In *International conference on machine learning*, pp. 10181–10192. PMLR, 2020.
- Williams, R. J. Simple statistical gradient-following algorithms for connectionist reinforcement learning. *Machine learning*, 8(3):229–256, 1992.
- Xie, C., Huang, Y., Zhang, C., Yu, D., Chen, X., Lin, B. Y., Li, B., Ghazi, B., and Kumar, R. On memorization of large language models in logical reasoning. *arXiv preprint arXiv:2410.23123*, 2024.
- Xie, T., Gao, Z., Ren, Q., Luo, H., Hong, Y., Dai, B., Zhou, J., Qiu, K., Wu, Z., and Luo, C. Logic-rl: Unleashing llm reasoning with rule-based reinforcement learning. *arXiv preprint arXiv:2502.14768*, 2025.
- Xing, X., Zhan, Q., Xie, X., Yang, Y., Wang, Q., and Liu, G. Flexible sharpness-aware personalized federated learning. In *Proceedings of the AAAI Conference on Artificial Intelligence*, volume 39, pp. 21707–21715, 2025.
- Xue, Z., Wu, J., Gao, Y., Kong, F., Zhu, L., Chen, M., Liu, Z., Liu, W., Guo, Q., Huang, W., et al. Dancegpro: Unleashing grpq on visual generation. *arXiv preprint arXiv:2505.07818*, 2025.

- Yang, A., Li, A., Yang, B., Zhang, B., Hui, B., Zheng, B., Yu, B., Gao, C., Huang, C., Lv, C., et al. Qwen3 technical report. *arXiv preprint arXiv:2505.09388*, 2025a.
- Yang, A., Yu, B., Li, C., Liu, D., Huang, F., Huang, H., Jiang, J., Tu, J., Zhang, J., Zhou, J., et al. Qwen2.5-1m technical report. *arXiv preprint arXiv:2501.15383*, 2025b.
- Yang, Z., Qi, P., Zhang, S., Bengio, Y., Cohen, W. W., Salakhutdinov, R., and Manning, C. D. Hotpotqa: A dataset for diverse, explainable multi-hop question answering. *arXiv preprint arXiv:1809.09600*, 2018.
- Yang, Z., Luo, X., Wang, Z., Han, D., He, Z., Li, D., and Xu, Y. Do not let low-probability tokens over-dominate in rl for llms. *arXiv preprint arXiv:2505.12929*, 2025c.
- Yu, Q., Zhang, Z., Zhu, R., Yuan, Y., Zuo, X., Yue, Y., Dai, W., Fan, T., Liu, G., Liu, L., et al. Dapo: An open-source llm reinforcement learning system at scale. *arXiv preprint arXiv:2503.14476*, 2025.
- Yue, Y., Yuan, Y., Yu, Q., Zuo, X., Zhu, R., Xu, W., Chen, J., Wang, C., Fan, T., Du, Z., et al. Vapo: Efficient and reliable reinforcement learning for advanced reasoning tasks. *arXiv preprint arXiv:2504.05118*, 2025.
- Zeng, W., Huang, Y., Liu, Q., Liu, W., He, K., Ma, Z., and He, J. Simplerl-zoo: Investigating and taming zero reinforcement learning for open base models in the wild. *arXiv preprint arXiv:2503.18892*, 2025.
- Zhao, A., Wu, Y., Yue, Y., Wu, T., Xu, Q., Lin, M., Wang, S., Wu, Q., Zheng, Z., and Huang, G. Absolute zero: Reinforced self-play reasoning with zero data. *arXiv preprint arXiv:2505.03335*, 2025.
- Zheng, C., Dang, K., Yu, B., Li, M., Jiang, H., Lin, J., Liu, Y., Yang, A., Zhou, J., and Lin, J. Stabilizing reinforcement learning with llms: Formulation and practices. *arXiv preprint arXiv:2512.01374*, 2025. URL <https://arxiv.org/abs/2512.01374>.
- Zhuang, J., Gong, B., Yuan, L., Cui, Y., Adam, H., Dvornek, N. C., Tatikonda, S., Duncan, J. S., and Liu, T. Surrogate gap minimization improves sharpness aware training. In *International Conference on Learning Representations (ICLR)*, 2022. URL <https://arxiv.org/abs/2203.08065>.

A. Related Work

Large-Scale Reasoning Models. Large language models (LLMs) (Lambert et al., 2024; Gao et al., 2024; Team et al., 2025; Guo et al., 2025; Yang et al., 2025a) have recently made substantial advances across a wide range of NLP tasks. A growing line of work now targets stronger performance in reasoning-intensive settings, including mathematics (Cobbe et al., 2021; Hendrycks et al., 2024), coding (Jain et al., 2024), and scientific reasoning (Rein et al., 2024). rStar-Math (Guan et al., 2025) introduces a self-evolving deep-thinking strategy that markedly improves the reasoning ability of smaller LLMs. OpenAI’s O-series (Jaech et al., 2024) scales reinforcement learning to train models that solve challenging reasoning problems and achieves state-of-the-art results on several benchmarks.

Reinforcement Learning for Large Language Model. Before reasoning-centric systems such as OpenAI’s O-series (Jaech et al., 2024), reinforcement learning (RL) was most commonly used through reinforcement learning from human feedback (RLHF) to improve instruction following and preference alignment in large language models (LLMs) (Ouyang et al., 2022). RLHF methods are often grouped into online and offline optimization. Online approaches, such as PPO (Schulman et al., 2017), GRPO (Shao et al., 2024), and REINFORCE (Williams, 1992), update the policy by sampling model outputs during training and optimizing against immediate reward signals. Offline approaches, including DPO (Rafailov et al., 2023), SimPO (Meng et al., 2024), and KTO (Ethayarajh et al., 2024), learn from pre-collected preference data provided by annotators or LLMs. Although offline training is typically more efficient, it often underperforms online RL in final capability (Tang et al., 2024). More recently, reinforcement learning with verifiable rewards (RLVR) has emerged as a promising route to strengthen LLM reasoning, especially for mathematics and programming. OpenAI o1 (Jaech et al., 2024) provided an early demonstration that RL can scale reasoning ability, and later systems such as DeepSeek-R1 (Guo et al., 2025), Kimi-2 (Team et al., 2025), and Qwen3 (Yang et al., 2025a) have matched or exceeded its performance. In particular, DeepSeek-R1 emphasizes that strong reasoning can arise from outcome-based online RL, notably with GRPO (Shao et al., 2024). These results also motivated “zero RL” directions that aim to elicit reasoning directly from base models without explicit RL fine-tuning, with follow-up methods including DAPO (Yu et al., 2025), VAPO (Yue et al., 2025), SimpleRLZoo (Zeng et al., 2025), and Open-Reasoner-Zero (Hu et al., 2025). In parallel, AR-Lopti (Yang et al., 2025c) shows that low-probability tokens can over-dominate GRPO-style RL updates, and mitigates this via advantage reweighting and low-probability token isolation.

Sharpness Aware Minimization. The relationship between wider, flatter minima and strong generalization has been widely investigated, with both theoretical analyses and empirical evidence reported across many studies (Tan et al., 2025; Jiang et al., 2020; Petzka et al., 2021; Dziugaite & Roy, 2017; Zhuang et al., 2022; Kwon et al., 2021). A common conclusion is that converging to flatter solutions can reduce generalization error and improve robustness under distribution shifts in a range of settings (Jiang et al., 2020; Petzka et al., 2021; Huang et al., 2025). Prior work has also examined how training choices such as batch size, learning rate, gradient covariance, and dropout influence the flatness of the attained minima (Keskar et al., 2017; Jastrzebski et al., 2017; Wei et al., 2020; Deng et al., 2025). Sharpness-Aware Minimization (SAM) (Foret et al., 2021) is a more recent optimization approach that targets improved generalization by explicitly accounting for loss-landscape sharpness during training. In particular, SAM optimizes the worst-case loss within a neighborhood of the current parameters, which encourages updates toward flatter regions while maintaining low training loss and better performance on unseen data. SAM has been applied successfully in diverse contexts, including vision (Chen et al., 2021), language modeling (Bahri et al., 2022), federated learning (Qu et al., 2022; Xing et al., 2025), Bayesian neural networks (Nguyen et al., 2023), domain generalization (Cha et al., 2021), multi-task learning (Phan et al., 2022), and bilevel meta-learning optimization (Abbas et al., 2022).

B. Implementation Details

B.1. Experiments setup

This appendix provides complete details of datasets, prompts, reward design, rollout/training configurations, and evaluation protocols for all three RLVR settings used in this paper: **Math reasoning**, **Agentic (VT-Search)** and **Logic (K&K)**.

B.1.1. MATH-RELATED DATASET

As mentioned in Section 4.1, inspired by (Yang et al., 2025c), we carry out additional experiments on two math-focused datasets, DSR-Uniform (10,000 problems, evenly covering difficulty levels) and ORZ (57,000 problems). In line with prior

studies, we adopt Qwen2.5-7B (Yang et al., 2025a) as the base model. In this setting, no instruction-tuned templates are applied; instead, we employ a simple prompt directly.

Prompt

{problem} Let’s think step by step and output the final answer within `\boxed{ }`.

LLMs without post-training generally struggle to follow strict output formats. Consequently, format-related signals are not included during training. Moreover, math tasks usually admit only a single correct solution, making partial credit unnecessary. Hence, a binary reward scheme is sufficient: the model receives a reward of 1 for a correct answer and 0 otherwise.

B.1.2. AGENTIC: VT-SEARCH (KNOWLEDGE-AUGMENTED QA)

Question answering tasks frequently demand access to external knowledge that goes beyond a model’s parametric memory, especially for factual queries and multi-hop reasoning. To address this, we follow the **Search-R1** (Jin et al., 2025) configuration from **VerlTool** framework (Jiang et al., 2025) which incorporates a FAISS-based retrieval module, allowing agents to query a local knowledge base and extract the most relevant evidence for answering complex questions.

Building on prior work (Jin et al., 2025; Song et al., 2025), an E5 retriever (Wang et al., 2022) was employed with the 2018 Wikipedia dump (Karpukhin et al., 2020) as the indexed corpus. The agent alternates between retrieval operations and reasoning steps to form complete answers. we adopt Qwen2.5-3B (Yang et al., 2025a) and Qwen3-4B-Instruct-2507 (Yang et al., 2025a) as the base models.

For this task, we use accuracy as the main reward, defined as:

$$R_{\text{search}}(\mathbf{x}, \mathbf{y}) = \begin{cases} 1 & \text{if match}(\mathbf{y}, \mathbf{y}_g) \\ -1 & \text{otherwise} \end{cases} \quad (20)$$

For evaluation, we follow the VerlTool benchmark and report exact-match scores on both General Q&A benchmarks (NQ (Kwiatkowski et al., 2019), TriviaQA (Joshi et al., 2017), PopQA (Mallen et al., 2022)) and multi-hop Q&A benchmark (HotpotQA (Yang et al., 2018), 2Wiki (Ho et al., 2020), MuSiQue (Trivedi et al., 2022), Bamboogle (Press et al., 2022))

B.1.3. LOGIC: KNIGHTS & KNAVES (K&K)

Following (Xie et al., 2025; Yang et al., 2025c), we adopt LLMs after instruction fine-tuning (Qwen2.5-3B-Instruct (Yang et al., 2025a) and Qwen2.5-7B-Instruct-1M (Yang et al., 2025b)) as the initialization point. The tailored prompt designed for the LLMs is provided below.

Prompt

system\n You are a helpful assistant. The assistant first thinks about the reasoning process in the mind and then provides the user with the answer. The reasoning process and answer are enclosed within `<think></think>` and `<answer></answer>` tags, respectively, i.e., `<think> reasoning process here </think><answer> answer here </answer>`. Now the user asks you to solve a logical reasoning problem. After thinking, when you finally reach a conclusion, clearly state the identity of each character within `<answer></answer>` tags. i.e., `<answer> (1) Zoey is a knight\n (2) ... </answer>`. \n user\n {problem} \n assistant\n <think>

To promote chain-of-thought (CoT) reasoning in LLMs, (Xie et al., 2025) introduces a reward function with two main components, as shown in Table 5. The output is judged as fully correct if the LLMs generate CoT reasoning wrapped inside `<think>...</think>` tags, and the final prediction enclosed within `<answer>...</answer>` tags.

B.2. Hyperparameters

The main GRPO hyperparameter settings are summarized in Table 6. The *clip-higher* technique from DAPO (Yu et al., 2025) is used to stabilize entropy and avoid collapse. Checkpoints are written every 20 RL steps, and the complete implementation is provided in the code release. For token importance estimation (Eq. 19), the configuration uses ($\alpha = 2.0$) and ($\mu = 0.25$),

Table 5. Reward design for Logic (K&K).

	Format Reward	Answer Reward
Completely Correct	1	2
Partially Correct	-1	-1.5
Completely Wrong	-1	-2

with clipping bounds ($L = 1.0$) and ($U = 1.4$), and the scaling parameter fixed to ($\tau = 9.0$). All experiments run on 8 NVIDIA H100 GPUs.

Table 6. Key hyperparameters for GRPO training.

Hyperparameter	Math reasoning	Agentic (Search-R1)	Logic (K&K)
Group size per prompt G	8	8	8
Sampling temperature	1.0	0.8	0.7
Max response length	4096	4096	4096
Optimizer / LR	AdamW / 1×10^{-6}	AdamW / 1×10^{-6}	AdamW / 1×10^{-6}
KL penalty coefficient	0.001	0.001	0.001
PPO clip ratio (low / high)	0.20 / 0.24	0.20 / 0.24	0.20 / 0.24
Mini-batch size	128	32	64
Micro-batch size (updates)	512	256	256

C. Additional Experiment Results

C.1. Hyperparameter sensitivity analysis

In Eq. 19, the token weight is determined by five hyperparameters: α , μ , L , U , and τ . Among these, α and μ mainly control the global mean of the weight distribution. Since the sigmoid term $\sigma(\text{sg}[\pi_{\theta}(o_{i,t} | q, o_{i,<t})]/\tau)$ lies in $(0.5, 1)$, we fix $\alpha = 2$ and $\mu = 0.25$, resulting in a centered range $(0.5, 1.5)$ with mean value close to 1.0. This ensures that token weights remain stable around unity, while still allowing enough variation to emphasize or de-emphasize tokens depending on their probability.

We then validate the two remaining hyperparameters, τ and the clipping range (L, U) . Table 7 reports results on the K&K Logic Puzzles benchmark using Qwen2.5-3B-Instruct. For τ , we sweep across $[0.5, 2.0, 7.0, 9.0, 10.0, 20.0]$. As τ increases, the weighting function becomes flatter and the weights tend to be nearly identical, making our method less effective. In contrast, very small τ produces overly sharp and highly disparate weights, which can amplify per-token variance and destabilize training. We observe the best performance at a moderate value around $\tau = 9.0$.

For (L, U) , we consider four ranges: $(1.0, 1.2)$, $(1.0, 1.4)$, $(0.8, 1.5)$, and $(0.5, 1.5)$. The choice of clipping bounds has only a mild effect, and all settings achieve comparable performance. This suggests that the precise clipping range mainly acts as a safeguard against extreme values rather than a critical tuning factor.

C.2. Cross-Model Validation

Beyond the Qwen family used in previous experiments, which is widely adopted in recent reasoning work, we further validate GRPO-SG on other model families, including Mistral and LLaMA. In addition, we test on the base variant Qwen2.5-3B-Base rather than the commonly used instruction-tuned variant. All evaluations follow the K&K logic setting, with results summarized in Table 8.

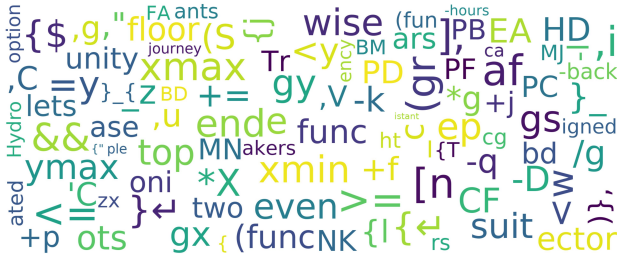
Table 8 shows that GRPO-SG consistently improves over GRPO across all tested backbones, indicating that our method generalizes beyond Qwen-Instruct models. This provides further evidence that the proposed token-weighted strategy is broadly applicable and not limited to a single model family.

Table 7. Hyperparameter sensitivity of token weight estimation on Qwen2.5-3B-Instruct on the K&K Logic Puzzles benchmark.

Parameter	Value	3	4	5	6	7	Avg.
τ	0.5	0.63	0.48	0.35	0.31	0.20	0.39
	2.0	0.64	0.49	0.37	0.33	0.19	0.40
	7.0	0.67	0.62	0.41	0.37	0.24	0.46
	9.0	0.76	0.76	0.61	0.59	0.44	0.63
	10.0	0.77	0.79	0.58	0.57	0.37	0.62
	20.0	0.74	0.68	0.51	0.46	0.35	0.55
(L, U)	(1.0, 1.2)	0.77	0.76	0.60	0.58	0.40	0.62
	(1.0, 1.4)	0.76	0.76	0.61	0.59	0.44	0.63
	(0.8, 1.5)	0.74	0.75	0.57	0.62	0.42	0.62
	(0.5, 1.5)	0.70	0.65	0.59	0.60	0.44	0.60

C.3. Visualize word cloud for top high and token

Our method assigns each token a weight that increases with its log-probability under the current policy: tokens with higher log-probability receive higher weights, and tokens with lower log-probability receive lower weights. To check whether this weighting mechanism aligns with semantic importance, we visualize the top 100 frequent high probability tokens and low-probability tokens ranked by their average model probability $\bar{\pi}(o_t) = \frac{1}{\#occ(o_t)} \sum_{o_t} \pi_{\theta}(o_t)$ (Figures 3a–3b) where $\#occ(o_t)$ denotes the number of occurrences of token o_t . Figure 3a shows that high-probability tokens concentrate on mathematical and logical *structure*—operators, brackets, variable names, and formatting markers—where even a single error can break the entire solution, whereas low-probability tokens are mostly generic content words (e.g., “output,” “particular,” “location”) that contribute less to the core reasoning and are more easily replaced without changing meaning. This creates a clear tension: standard GRPO naturally magnifies low-probability tokens (via larger gradients) even though high-probability tokens carry the most critical signal for correctness. This analysis further support for our method.



(a) Frequent tokens with the highest average probability.



(b) Frequent tokens with the lowest average probability.

Figure 3. Word clouds of the top 100 high- vs. low-probability tokens selected from frequently occurring words. High-probability tokens (left) primarily consist of mathematical and logical operators, brackets, and variable names, where even small errors can invalidate an entire solution, whereas low-probability tokens (right) mostly consist of generic content words that are less critical.

C.4. Ablation on Probability-Based Token Weighting

In addition to the main experiments, we compare: (i) GRPO-SG, which applies our probability-aware token weighting rule; (ii) a Reverse variant that flips this rule by assigning $2 - w$ to any token whose GRPO-SG weight is w ; and (iii) the GRPO baseline, which does not use token-level weights. GRPO-SG, which applies our probability-aware token weighting rule. As shown in Figure 4, **GRPO-SG (blue)** consistently outperforms both **Reverse (orange)** and the **GRPO baseline (green)** across K&K puzzle sizes (3–7), while Reverse tracks GRPO closely without clear improvement. Beyond accuracy, this ablation supports our generalization view: GRPO-SG yields a more stable performance trajectory, while GRPO and the Reverse variant exhibit larger fluctuations.

Table 8. Experimental results on the K&K Logic Puzzles benchmark on various models. The best results are indicated in **bold**.

Model	Difficulty by Number of People					Avg.	
	3	4	5	6	7		
Qwen2.5-3B-Instruct	0.09	0.10	0.03	0.05	0.02	0.06	
+ GRPO	0.64	0.47	0.35	0.30	0.21	0.39	
+ GRPO-SG	0.76	0.76	0.61	0.59	0.44	0.63	↑ 61.5%
Qwen2.5-7B-Instruct-1M	0.22	0.15	0.08	0.10	0.02	0.11	
+ GRPO	0.91	0.91	0.77	0.65	0.61	0.77	
+ GRPO-SG	0.95	0.95	0.92	0.87	0.84	0.91	↑ 18.2%
Qwen2.5-3B-Base	0.14	0.04	0.02	0.01	0.02	0.05	
+ GRPO	0.60	0.54	0.43	0.38	0.28	0.45	
+ GRPO-SG	0.68	0.62	0.44	0.47	0.26	0.49	↑ 8.9%
Mistral-7B-Instruct-v0.3	0.05	0.01	0.00	0.02	0.00	0.02	
+ GRPO	0.29	0.16	0.09	0.11	0.03	0.14	
+ GRPO-SG	0.47	0.27	0.18	0.15	0.08	0.23	↑ 64.3%
LLaMa3.1-8B-Instruct	0.08	0.00	0.00	0.00	0.00	0.02	
+ GRPO	0.92	0.92	0.83	0.79	0.80	0.85	
+ GRPO-SG	0.89	0.95	0.88	0.87	0.81	0.88	↑ 3.5%

D. Proof of Our Theories

D.1. Proof of Lemma 3.1

We have

$$\pi_* = \operatorname{argmax}_{\pi} \left\{ \mathbb{E}_q \left[\sum_{t=1}^{|\mathcal{O}|} \mathbb{E}_{o_t \sim \pi(\cdot | q, o_{<t})} [r_*([q, o_{<t}], o_t)] \right] - \lambda \sum_{t=1}^{|\mathcal{O}|} D_f(\pi(\cdot | q, o_{<t}) \| \pi_{old}(\cdot | q, o_{<t})) \right\}, \quad (21)$$

For $t \leq T$, we investigate

$$\max_{\pi} \mathbb{E}_q [\pi(o_t | q, o_{<t}) r_*([q, o_{<t}], o_t)] - \lambda D_f(\pi(\cdot | q, o_{<t}) \| \pi_{old}(\cdot | q, o_{<t})). \quad (22)$$

We construct the Lagrange function

$$\begin{aligned} \mathcal{L}(\pi, \beta, \alpha) = & \mathbb{E}_q [\pi(o_t | q, o_{<t}) r_*([q, o_{<t}], o_t)] - \sum_{o_t} f \left(\frac{\pi(o_t | q, o_{<t})}{\pi_{old}(o_t | q, o_{<t})} \right) \pi_{old}(o_t | q, o_{<t}) \\ & + \sum_{o_t} \alpha(o_t) \pi(o_t | q, o_{<t}) + \beta \left(\sum_{o_t} \pi(o_t | q, o_{<t}) - 1 \right). \end{aligned}$$

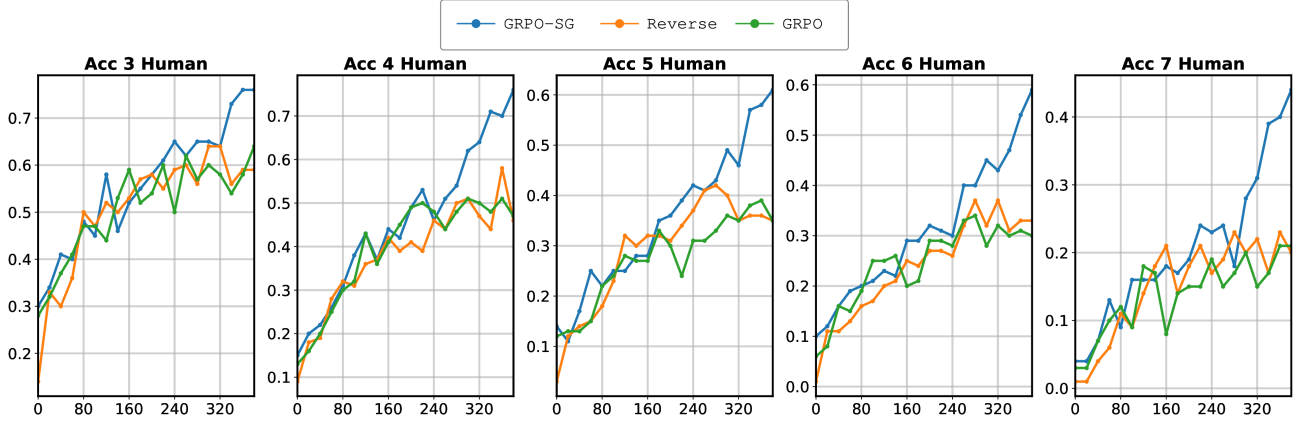


Figure 4. Accuracy on the K&K Logic Puzzles benchmark, broken down by puzzle size (3–7 people). GRPO-SG consistently achieves higher accuracy than GRPO across all difficulty levels, while the Reverse variant yields performance comparable to GRPO without clear improvement.

Using KKT conditions, we have

$$\begin{aligned} \frac{d\mathcal{L}}{d\pi(o_t | q, o_{<t})} &= r_*([q, o_{<t}], o_t) - \lambda f' \left(\frac{\pi(o_t | q, o_{<t})}{\pi_{old}(o_t | q, o_{<t})} \right) + \alpha(o_t) + \beta = 0 \\ \sum_{o_t} \pi(o_t | q, o_{<t}) - 1 &= 0 \\ \sum_{o_t} \alpha(o_t) &\geq 0, \alpha(o_t) \pi(o_t | q, o_{<t}) = 0 \end{aligned}$$

We have $\pi(o_t | q, o_{<t}) > 0$, leading to $\alpha(o_t) = 0$ and

$$r_*([q, o_{<t}], o_t) = \lambda f' \left(\frac{\pi(o_t | q, o_{<t})}{\pi_{old}(o_t | q, o_{<t})} \right) - \beta = \lambda f' \left(\frac{\pi(o_t | q, o_{<t})}{\pi_{old}(o_t | q, o_{<t})} \right) + const.$$

By choosing

$$f(t) = \lambda^{-1} \int_0^t \frac{\omega(x\pi_{old}(o_t))}{\pi_{old}(o_t)} dx,$$

we have f is convex and $f'(t) = \lambda^{-1} \frac{\omega(t\pi_{old}(o_t))}{\pi_{old}(o_t)}$.

Finally, consider $t = \frac{\pi_*(o_t)}{\pi_{old}(o_t)}$, we reach

$$r_*([q, o_{<t}], o_t) = \lambda f' \left(\frac{\pi(o_t)}{\pi_{old}(o_t)} \right) + const = \frac{\omega(\pi_*(o_t))}{\pi_{old}(o_t)} + const$$

D.2. Proof of Theorem 3.2

We consider

$$\begin{aligned} \max_{\theta} \mathbb{E}_{\mathcal{Q}} \left[\frac{1}{|o|} \sum_{t=1}^{|o|} \mathbb{E}_{o_{\leq t} \sim \pi_*^{(-|q|)}} \left[\omega(\pi_*(o_t)) \frac{\pi_{\theta}(o_t)}{\pi_{old}(o_t)} \right] \right] \\ - \beta \mathbb{D}_{KL}(\pi_{\theta} \| \pi_{ref}). \end{aligned} \quad (23)$$

We rewrite the first term in the objective function as

$$\begin{aligned}
 & \mathbb{E}_{\mathcal{Q}} \left[\frac{1}{|o|} \sum_{t=1}^{|o|} \mathbb{E}_{o_{\leq t} \sim \pi_*^t(\cdot|q)} \left[\omega(\pi_*(o_t)) \frac{\pi_{\theta}(o_t)}{\pi_{old}(o_t)} \right] \right] \\
 &= \mathbb{E}_{\mathcal{Q}} \left[\frac{1}{|o|} \sum_{t=1}^{|o|} \sum_{o_{\leq t}} \pi_*^t(o_{\leq t} | q) \omega(\pi_*(o_t)) \frac{\pi_{\theta}(o_t)}{\pi_{old}(o_t)} \right] \\
 &= \mathbb{E}_{\mathcal{Q}} \left[\frac{1}{|o|} \sum_{t=1}^{|o|} \sum_{o_{\leq t}} \pi_{old}^t(o_{\leq t} | q) \omega(\pi_{\theta}(o_t)) \frac{\pi_{\theta}(o_t)}{\pi_{old}(o_t)} \right] \\
 &+ \mathbb{E}_{\mathcal{Q}} \left[\frac{1}{|o|} \sum_{t=1}^{|o|} \sum_{o_{\leq t}} [\pi_*^t(o_{\leq t} | q) - \pi_{old}^t(o_{\leq t} | q)] \omega(\pi_*(o_t)) \frac{\pi_{\theta}(o_t)}{\pi_{old}(o_t)} \right] \\
 &+ \mathbb{E}_{\mathcal{Q}} \left[\frac{1}{|o|} \sum_{t=1}^{|o|} \sum_{o_{\leq t}} \pi_{old}^t(o_{\leq t} | q) [\omega(\pi_*(o_t)) - \omega(\pi_{\theta}(o_t))] \frac{\pi_{\theta}(o_t)}{\pi_{old}(o_t)} \right]. \tag{24}
 \end{aligned}$$

We further bound

$$\begin{aligned}
 & \mathbb{E}_{\mathcal{Q}} \left[\frac{1}{|o|} \sum_{t=1}^{|o|} \sum_{o_{\leq t}} (\pi_*^t(o_{\leq t} | q) - \pi_{old}^t(o_{\leq t} | q)) \omega(\pi_*(o_t)) \frac{\pi_{\theta}(o_t)}{\pi_{old}(o_t)} \right] \\
 &\leq \mathbb{E}_{\mathcal{Q}} \left[\frac{1}{|o|} \sum_{t=1}^{|o|} \left\{ \sum_{o_{\leq t}} \frac{\pi_*^t(o_{\leq t} | q) - \pi_{old}^t(o_{\leq t} | q)}{\pi_*^t(o_{\leq t} | q)} \pi_*^t(o_{\leq t} | q)^{1/2} \right\} \left\{ \pi_*^t(o_{\leq t} | q)^{1/2} \omega(\pi_*(o_t)) \frac{\pi_{\theta}(o_t)}{\pi_{old}(o_t)} \right\} \right] \\
 &\stackrel{(1)}{\leq} \mathbb{E}_{\mathcal{Q}} \left[\frac{1}{|o|} \sum_{t=1}^{|o|} \left\{ \sum_{o_{\leq t}} \pi_*^t(o_{\leq t} | q) \left(\frac{\pi_*^t(o_{\leq t} | q) - \pi_{old}^t(o_{\leq t} | q)}{\pi_*^t(o_{\leq t} | q)} \right)^2 \right\}^{\frac{1}{2}} \left\{ \sum_{o_{\leq t}} \pi_*^t(o_{\leq t} | q) \omega^2(\pi_*(o_t)) \left(\frac{\pi_{\theta}(o_t)}{\pi_{old}(o_t)} \right)^2 \right\}^{\frac{1}{2}} \right] \\
 &\leq A \mathbb{E}_{\mathcal{Q}} \left[\frac{1}{|o|} \sum_{t=1}^{|o|} D_u(\pi_{old}^t(o_{\leq t} | q) \| \pi_*^t(o_{\leq t} | q))^{\frac{1}{2}} \left(\sum_{o_{\leq t}} \pi_*^t(o_{\leq t} | q) \left(\frac{\pi_{\theta}(o_t)}{\pi_{old}(o_t)} \right)^2 \right)^{\frac{1}{2}} \right] \\
 &= \mathbb{E}_{\mathcal{Q}} \left[\frac{1}{|o|} \sum_{t=1}^{|o|} d(\pi_{old}^t, \pi_*^t) \right], \tag{25}
 \end{aligned}$$

where in $\stackrel{(1)}{\leq}$, we use Cauchy-Schwarz inequality, D_u is a f -divergence with $u(t) = (t-1)^2$, A is an upper-bound of $|\omega(\cdot)|$, and we define

$$d(\pi_{old}^t, \pi_*^t) = A \left(\sum_{o_{\leq t}} \pi_*^t(o_{\leq t} | q) \left(\frac{\pi_{\theta}(o_t)}{\pi_{old}(o_t)} \right)^2 \right)^{\frac{1}{2}} D_u(\pi_{old}^t(o_{\leq t} | q) \| \pi_*^t(o_{\leq t} | q))^{\frac{1}{2}}.$$

$$\begin{aligned}
 & \mathbb{E}_Q \left[\frac{1}{|O|} \sum_{t=1}^{|O|} \sum_{o \leq t} \pi_{old}^t(o \leq t | q) [\omega(\pi_*(o_t)) - \omega(\pi_\theta(o_t))] \frac{\pi_\theta(o_t)}{\pi_{old}(o_t)} \right] \\
 &= \mathbb{E}_Q \left[\frac{1}{|O|} \sum_{t=1}^{|O|} \left\{ \sum_{o \leq t} \pi_{old}^t(o \leq t | q)^{\frac{1}{2}} [\omega(\pi_*(o_t)) - \omega(\pi_\theta(o_t))] \right\} \left\{ \sum_{o \leq t} \pi_{old}^t(o \leq t | q)^{\frac{1}{2}} \frac{\pi_\theta(o_t)}{\pi_{old}(o_t)} \right\} \right] \\
 &\stackrel{(2)}{\leq} \mathbb{E}_Q \left[\frac{1}{|O|} \sum_{t=1}^{|O|} \left[\sum_{o \leq t} \pi_{old}^t(o \leq t | q) [\omega(\pi_*(o_t)) - \omega(\pi_\theta(o_t))]^2 \right]^{\frac{1}{2}} \left[\sum_{o \leq t} \pi_{old}^t(o \leq t | q) \left(\frac{\pi_\theta(o_t)}{\pi_{old}(o_t)} \right)^2 \right]^{\frac{1}{2}} \right] \\
 &= \mathbb{E}_Q \left[\frac{1}{|O|} \sum_{t=1}^{|O|} d'(\pi_*, \pi_\theta^t) \right], \tag{26}
 \end{aligned}$$

where in $\stackrel{(2)}{\leq}$, we use Cauchy-Schwarz inequality and we define

$$d'(\pi_*, \pi_\theta^t) = \left[\sum_{o \leq t} \pi_{old}^t(o \leq t | q) \left(\frac{\pi_\theta(o_t)}{\pi_{old}(o_t)} \right)^2 \right]^{\frac{1}{2}} \left[\sum_{o \leq t} \pi_{old}^t(o \leq t | q) [\omega(\pi_*(o_t)) - \omega(\pi_\theta(o_t))]^2 \right]^{\frac{1}{2}}.$$

Combining (24), (25), and (26), we reach the conclusion.

D.3. Proof of Theorem 3.3

We use the PAC-Bayes theory in this proof. In PAC-Bayes theory, θ could follow a distribution, says P , thus we define the expected loss over θ distributed by P as follows:

$$\begin{aligned}
 \mathcal{L}_D(\theta, P) &= \mathbb{E}_{\theta \sim P} [\mathcal{L}_D(\theta)] \\
 \mathcal{L}_S(\theta, P) &= \mathbb{E}_{\theta \sim P} [\mathcal{L}_S(\theta)].
 \end{aligned}$$

For any distribution $P = \mathcal{N}(\mathbf{0}, \sigma_P^2 \mathbb{I}_k)$ and $Q = \mathcal{N}(\theta, \sigma^2 \mathbb{I}_k)$ over $\theta \in \mathbb{R}^k$, where P is the prior distribution and Q is the posterior distribution, use the PAC-Bayes theorem in (Alquier et al., 2016), for all $\beta > 0$, with a probability at least $1 - \delta$, we have

$$\mathcal{L}_D(\theta, Q) \leq \mathcal{L}_S(\theta, Q) + \frac{1}{\beta} \left[\text{KL}(Q \| P) + \log \frac{1}{\delta} + \Psi(\beta, N) \right], \tag{27}$$

where Ψ is defined as

$$\Psi(\beta, N) = \log \mathbb{E}_P \mathbb{E}_{\mathcal{D}^N} \left[\exp \left\{ \beta [\mathcal{L}_D(f_\theta) - \mathcal{L}_S(f_\theta)] \right\} \right].$$

When the loss function is bounded by L , then

$$\Psi(\beta, N) \leq \frac{\beta^2 L^2}{8N}.$$

The task is to minimize the second term of RHS of equation 27, we thus choose $\beta = \sqrt{8N \frac{\text{KL}(Q \| P) + \log \frac{1}{\delta}}{L}}$. Then the second term of RHS of equation 27 is equal to

$$\sqrt{\frac{\text{KL}(Q \| P) + \log \frac{1}{\delta}}{2N}} \times L.$$

The KL divergence between Q and P , when they are Gaussian, is given by formula

$$\text{KL}(Q \| P) = \frac{1}{2} \left[\frac{k\sigma^2 + \|\theta\|^2}{\sigma_P^2} - k + k \log \frac{\sigma_P^2}{\sigma^2} \right].$$

For given posterior distribution Q with fixed σ^2 , to minimize the KL term, the σ_P^2 should be equal to $\sigma^2 + \|\theta\|^2/k$. In this case, the KL term is no less than

$$k \log \left(1 + \frac{\|\theta_0\|^2}{k\sigma^2} \right).$$

Thus, the second term of RHS is

$$\sqrt{\frac{\text{KL}(Q\|P) + \log \frac{1}{\delta}}{2N}} \times L \geq \sqrt{\frac{k \log \left(1 + \frac{\|\theta\|^2}{k\sigma^2} \right)}{4N}} \times L \geq L$$

when $\|\theta\|^2 > \sigma^2 \{ \exp(4N/k) - 1 \}$. Hence, for any $\|\theta\|_2 > \sigma^2 \{ \exp(4N/k) - 1 \}$, we have the RHS is greater than the LHS, and the inequality is trivial. In this work, we only consider the case:

$$\|\theta\|^2 < \sigma^2 (\exp\{4N/k\} - 1). \quad (28)$$

Distribution P is Gaussian centered around $\mathbf{0}$ with variance $\sigma_P^2 = \sigma^2 + \|\theta\|^2/k$, which is unknown at the time we set up the inequality, since θ is unknown. Meanwhile, we have to specify P in advance, since P is the prior distribution. To deal with this problem, we could choose a family of P such that its means cover the space of θ satisfying inequality equation 28. We set

$$\begin{aligned} c &= \sigma^2 (1 + \exp\{4N/k\}) \\ P_j &= \mathcal{N}(0, c \exp \frac{1-j}{k} \mathbb{I}_k) \\ \mathfrak{P} &:= \{P_j : j = 1, 2, \dots\} \end{aligned}$$

Then the following inequality holds for a particular distribution P_j with probability $1 - \delta_j$ with $\delta_j = \frac{6\delta}{\pi^2 j^2}$

$$\mathbb{E}_{\theta' \sim \mathcal{N}(\theta, \sigma^2)} \mathcal{L}_{\mathcal{D}}(f_{\theta'}) \leq \mathbb{E}_{\theta' \sim \mathcal{N}(\theta, \sigma^2)} \mathcal{L}_{\mathcal{S}}(f_{\theta'}) + \frac{1}{\beta} \left[\text{KL}(Q\|P_j) + \log \frac{1}{\delta_j} + \Psi(\beta, N) \right].$$

Use the well-known equation: $\sum_{j=1}^{\infty} \frac{1}{j^2} = \frac{\pi^2}{6}$, then with probability $1 - \delta$, the above inequality holds with every j . We pick

$$j^* := \left\lceil 1 - k \log \frac{\sigma^2 + \|\theta\|^2/k}{c} \right\rceil = \left\lceil 1 - k \log \frac{\sigma^2 + \|\theta\|^2/k}{\sigma^2(1 + \exp\{4N/k\})} \right\rceil.$$

Therefore,

$$\begin{aligned} 1 - j^* &= \left\lceil k \log \frac{\sigma^2 + \|\theta\|^2/k}{c} \right\rceil \\ \Rightarrow \log \frac{\sigma^2 + \|\theta\|^2/k}{c} &\leq \frac{1 - j^*}{k} \leq \log \frac{\sigma^2 + \|\theta\|^2/k}{c} + \frac{1}{k} \\ \Rightarrow \sigma^2 + \|\theta\|^2/k &\leq c \exp \left\{ \frac{1 - j^*}{k} \right\} \leq \exp(1/k) [\sigma^2 + \|\theta\|^2/k] \\ \Rightarrow \sigma^2 + \|\theta\|^2/k &\leq \sigma_{P_{j^*}}^2 \leq \exp(1/k) [\sigma^2 + \|\theta\|^2/k]. \end{aligned}$$

Thus the KL term could be bounded as follow

$$\begin{aligned} \text{KL}(Q\|P_{j^*}) &= \frac{1}{2} \left[\frac{k\sigma^2 + \|\theta\|^2}{\sigma_{P_{j^*}}^2} - k + k \log \frac{\sigma_{P_{j^*}}^2}{\sigma^2} \right] \\ &\leq \frac{1}{2} \left[\frac{k(\sigma^2 + \|\theta\|^2/k)}{\sigma^2 + \|\theta\|^2/k} - k + k \log \frac{\exp(1/k)(\sigma^2 + \|\theta\|^2/k)}{\sigma^2} \right] \\ &= \frac{1}{2} \left[k \log \frac{\exp(1/k)(\sigma^2 + \|\theta\|^2/k)}{\sigma^2} \right] \\ &= \frac{1}{2} \left[1 + k \log \left(1 + \frac{\|\theta_0\|^2}{k\sigma^2} \right) \right] \end{aligned}$$

For the term $\log \frac{1}{\delta_{j^*}}$, with recall that $c = \sigma^2(1 + \exp(4N/k))$ and $j^* = \left\lfloor 1 - k \log \frac{\sigma^2 + \|\theta\|^2/k}{\sigma^2(1 + \exp\{4N/k\})} \right\rfloor$, we have

$$\begin{aligned}
 \log \frac{1}{\delta_{j^*}} &= \log \frac{(j^*)^2 \pi^2}{6\delta} = \log \frac{1}{\delta} + \log \left(\frac{\pi^2}{6} \right) + 2 \log(j^*) \\
 &\leq \log \frac{1}{\delta} + \log \frac{\pi^2}{6} + 2 \log \left(1 + k \log \frac{\sigma^2(1 + \exp(4N/k))}{\sigma^2 + \|\theta\|^2/k} \right) \\
 &\leq \log \frac{1}{\delta} + \log \frac{\pi^2}{6} + 2 \log \left(1 + k \log(1 + \exp(4N/k)) \right) \\
 &\leq \log \frac{1}{\delta} + \log \frac{\pi^2}{6} + 2 \log \left(1 + k \left(1 + \frac{4N}{k} \right) \right) \\
 &\leq \log \frac{1}{\delta} + \log \frac{\pi^2}{6} + \log(1 + k + 4N).
 \end{aligned}$$

Hence, the inequality

$$\begin{aligned}
 \mathcal{L}_{\mathcal{D}}(\theta', \mathcal{N}(\theta, \sigma^2 \mathbb{I}_k)) &\leq \mathcal{L}_{\mathcal{S}}(\theta', \mathcal{N}(\theta, \sigma^2 \mathbb{I}_k)) + \sqrt{\frac{\text{KL}(Q \| P_{j^*}) + \log \frac{1}{\delta_{j^*}}}{2N}} \times L \\
 &\leq \mathcal{L}_{\mathcal{S}}(\theta', \mathcal{N}(\theta, \sigma^2 \mathbb{I}_k)) \\
 &\quad + \frac{L}{2\sqrt{N}} \sqrt{1 + k \log \left(1 + \frac{\|\theta\|^2}{k\sigma^2} \right) + 2 \log \frac{\pi^2}{6\delta} + 4 \log(N + k)} \\
 &\leq \mathcal{L}_{\mathcal{S}}(\theta', \mathcal{N}(\theta, \sigma^2 \mathbb{I}_k)) \\
 &\quad + \frac{L}{2\sqrt{N}} \sqrt{k \log \left(1 + \frac{\|\theta\|^2}{k\sigma^2} \right) + O(1) + 2 \log \frac{1}{\delta} + 4 \log(N + k)}.
 \end{aligned}$$

Since $\|\theta' - \theta\|^2$ is k chi-square distribution, for any positive t , we have

$$\mathbb{P}(\|\theta' - \theta\|^2 - k\sigma^2 \geq 2\sigma^2\sqrt{kt} + 2t\sigma^2) \leq \exp(-t).$$

By choosing $t = \frac{1}{2} \log(N)$, with probability $1 - N^{-1/2}$, we have

$$\|\theta' - \theta\|^2 \leq \sigma^2 \log(N) + k\sigma^2 + \sigma^2 \sqrt{2k \log(N)} \leq k\sigma^2 \left(1 + \sqrt{\frac{\log(N)}{k}} \right)^2.$$

By setting $\sigma = \rho \times (\sqrt{k} + \sqrt{\log(N)})^{-1}$, we have $\|\theta' - \theta\|^2 \leq \rho^2$. Hence, we get

$$\begin{aligned}
 \mathcal{L}_{\mathcal{S}}(\theta', \mathcal{N}(\theta, \sigma^2 \mathbb{I}_k)) &= \mathbb{E}_{\theta \sim \mathcal{N}(\theta, \sigma^2 \mathbb{I}_k)} \mathbb{E}_{\mathcal{S}}[f_{\theta'}] = \int_{\|\theta' - \theta\| \leq \rho} \mathbb{E}_{\mathcal{S}}[f_{\theta'}] d\mathcal{N}(\theta, \sigma^2 \mathbb{I}) \\
 &\quad + \int_{\|\theta' - \theta\| > \rho} \mathbb{E}_{\mathcal{S}}[f_{\theta'}] d\mathcal{N}(\theta, \sigma^2 \mathbb{I}) \\
 &\leq \left(1 - \frac{1}{\sqrt{N}} \right) \max_{\|\theta' - \theta\| \leq \rho} \mathcal{L}_{\mathcal{S}}(\theta') + \frac{1}{\sqrt{N}} L \\
 &\leq \max_{\|\theta' - \theta\|_2 \leq \rho} \mathcal{L}_{\mathcal{S}}(\theta') + \frac{2L}{\sqrt{N}}.
 \end{aligned}$$

It follows that

$$\begin{aligned}
 \mathcal{L}_{\mathcal{D}}(\theta) &\leq \max_{\|\theta' - \theta\| \leq \rho} \mathcal{L}_{\mathcal{S}}(\theta') + \frac{4L}{\sqrt{N}} \left[\sqrt{k \log \left(1 + \frac{\|\theta\|^2}{\rho^2} (1 + \sqrt{\log(N)/k})^2 \right)} \right. \\
 &\quad \left. + 2\sqrt{\log \left(\frac{N+k}{\delta} \right)} + O(1) \right] \\
 &= \mathcal{L}_{\mathcal{D}}(\theta | \mathcal{S}) + \frac{4L}{\sqrt{N}} \left[\sqrt{k \log \left(1 + \frac{\|\theta\|^2}{\rho^2} (1 + \sqrt{\log(N)/k})^2 \right)} \right. \\
 &\quad \left. + 2\sqrt{\log \left(\frac{N+k}{\delta} \right)} + O(1) \right].
 \end{aligned}$$

For our case, the loss is bounded by $(1 + \epsilon_h) \max \hat{A}_{i,t} \leq (1 + \epsilon_h) G^{1/2} = L$. The reason is that $\frac{1}{G} \sum_{i=1}^G \hat{A}_{i,t} = 0$ and $\frac{1}{G} \sum_{i=1}^G \hat{A}_{i,t}^2 = 1$.

D.4. Proof of Lemma 3.4

For $\hat{A}_{i,t} > 0$, the inner term of the sum relevant to $o_{i,t}$ reduces to

$$h(o_{i,t}) = \begin{cases} (1 + \epsilon_h) \hat{A}_{i,t} & w_{i,t} \frac{\pi_{\theta}(o_{i,t})}{\pi_{\text{old}}(o_{i,t})} > 1 + \epsilon_h \\ w_{i,t} \frac{\pi_{\theta}(o_{i,t})}{\pi_{\text{old}}(o_{i,t})} \hat{A}_{i,t} & w_{i,t} \frac{\pi_{\theta}(o_{i,t})}{\pi_{\text{old}}(o_{i,t})} \leq 1 + \epsilon_h \end{cases}$$

The derivative w.r.t. θ becomes

$$\nabla_{\theta} h(o_{i,t}) = \begin{cases} 0 & w_{i,t} \frac{\pi_{\theta}(o_{i,t})}{\pi_{\text{old}}(o_{i,t})} > 1 + \epsilon_h \\ w_{i,t} \frac{\pi_{\theta}(o_{i,t})}{\pi_{\text{old}}(o_{i,t})} \nabla_{\theta} \log \pi_{\theta}(o_{i,t}) \hat{A}_{i,t} & w_{i,t} \frac{\pi_{\theta}(o_{i,t})}{\pi_{\text{old}}(o_{i,t})} \leq 1 + \epsilon_h \end{cases}$$

Combining with the KL term derivative, we gain

$$\begin{aligned}
 &\nabla_{\theta} h(o_{i,t}) + \beta w_{i,t} \pi_{\text{ref}}(o_{i,t}) \frac{\nabla_{\theta} \pi_{\theta}(o_{i,t})}{\pi_{\theta}(o_{i,t})^2} - \beta w_{i,t} \nabla_{\theta} \log \pi_{\theta}(o_{i,t}) \\
 &= \nabla_{\theta} h(o_{i,t}) + \beta w_{i,t} \frac{\pi_{\text{ref}}(o_{i,t})}{\pi_{\theta}(o_{i,t})} \nabla_{\theta} \log \pi_{\theta}(o_{i,t}) - \beta w_{i,t} \nabla_{\theta} \log \pi_{\theta}(o_{i,t})
 \end{aligned}$$

For $\hat{A}_{i,t} < 0$, the inner term of the sum relevant to $o_{i,t}$ reduces to

$$h(o_{i,t}) = \begin{cases} (1 - \epsilon_l) \hat{A}_{i,t} & w_{i,t} \frac{\pi_{\theta}(o_{i,t})}{\pi_{\text{old}}(o_{i,t})} < 1 - \epsilon_l \\ w_{i,t} \frac{\pi_{\theta}(o_{i,t})}{\pi_{\text{old}}(o_{i,t})} \hat{A}_{i,t} & w_{i,t} \frac{\pi_{\theta}(o_{i,t})}{\pi_{\text{old}}(o_{i,t})} \geq 1 - \epsilon_l \end{cases}$$

The derivative w.r.t. θ becomes

$$\nabla_{\theta} h(o_{i,t}) = \begin{cases} 0 & w_{i,t} \frac{\pi_{\theta}(o_{i,t})}{\pi_{\text{old}}(o_{i,t})} < 1 - \epsilon_l \\ w_{i,t} \frac{\pi_{\theta}(o_{i,t})}{\pi_{\text{old}}(o_{i,t})} \nabla_{\theta} \log \pi_{\theta}(o_{i,t}) \hat{A}_{i,t} & w_{i,t} \frac{\pi_{\theta}(o_{i,t})}{\pi_{\text{old}}(o_{i,t})} \geq 1 - \epsilon_l \end{cases}$$

Combining with the KL term derivative, we gain

$$\begin{aligned}
 &\nabla_{\theta} h(o_{i,t}) + \beta w_{i,t} \pi_{\text{ref}}(o_{i,t}) \frac{\nabla_{\theta} \pi_{\theta}(o_{i,t})}{\pi_{\theta}(o_{i,t})^2} - \beta w_{i,t} \nabla_{\theta} \log \pi_{\theta}(o_{i,t}) \\
 &= \nabla_{\theta} h(o_{i,t}) + \beta w_{i,t} \frac{\pi_{\text{ref}}(o_{i,t})}{\pi_{\theta}(o_{i,t})} \nabla_{\theta} \log \pi_{\theta}(o_{i,t}) - \beta w_{i,t} \nabla_{\theta} \log \pi_{\theta}(o_{i,t})
 \end{aligned}$$

Finally, leveraging the two above cases, we gain the final formula.

Lemma D.1. Assume that $A_{1:m}$ is a sequence of matrices with $\sigma_{\min}(A_i) \geq a_i^2 \geq 0$ and $\sigma_{\max}(A_i) \leq b_i^2$ for all $i \in \{1, \dots, m\}$. We then have

$$\|x\|_2 \prod_{i=m}^1 a_i \leq \|x \prod_{i=m}^1 A_i\|_2 \leq \|x\|_2 \prod_{i=m}^1 b_i$$

Proof. We start with

$$\|xA\|_2^2 = xAA^T x^T.$$

According to the Rayleigh inequality, we have

$$\begin{aligned} \sigma_{\min}(A) \|x\|_2^2 &\leq \|xA\|_2^2 = xAA^T x^T \leq \sigma_{\max}(A) \|x\|_2^2 \\ \sigma_{\min}(A)^{1/2} \|x\|_2 &\leq \|xA\|_2 \leq \sigma_{\max}(A)^{1/2} \|x\|_2 \end{aligned} \quad (29)$$

Consider $A = \prod_{i=m}^1 A_i$ and apply Inequality 29 recursively, we obtain

$$\begin{aligned} \|x\|_2 \prod_{i=m}^1 \sigma_{\min}(A_i)^{1/2} &\leq \|x \prod_{i=m}^1 A_i\|_2 \leq \|x\|_2 \prod_{i=m}^1 \sigma_{\max}(A_i)^{1/2} \\ \|x\|_2 \prod_{i=m}^1 a_i &\leq \|x \prod_{i=m}^1 A_i\|_2 \leq \|x\|_2 \prod_{i=m}^1 b_i \end{aligned}$$

□

D.5. Proof of Theorem 3.5

We first have

$$\frac{\partial \log \pi_{\theta}(o_{i,t})}{\partial h_{i,t}} = \mathbf{1}_k - p_{i,t},$$

where $\mathbf{1}_k$ is a one-hot vector over the vocabulary, the token $o_{i,t}$ has the index k in the vocabulary, $p_{i,t}$ is the distribution over vocabulary with $\pi_{\theta}(o_{i,t}) = p_{i,t}(k)$.

Consider a specific layer l , we then have

$$\begin{aligned} \frac{\partial \log \pi_{\theta}(o_{i,t})}{\partial \theta_l} &= \frac{\partial \log \pi_{\theta}(o_{i,t})}{\partial h_{i,t}} \frac{\partial h_{i,t}}{\partial a_L} \frac{\partial a_L}{\partial a_{L-1}} \cdots \frac{\partial a_{l+1}}{\partial a_l} \frac{\partial a_l}{\partial \theta_l} \\ &= [\mathbf{1}_k - p_{i,t}] W \prod_{i=l}^L J_i G_l. \end{aligned}$$

Applying Lemma D.1, we reach

$$\|\mathbf{1}_k - p_{i,t}\|_2 a^W a_l^G \prod_{i=l}^L a_i^J \leq \left\| \frac{\partial \log \pi_{\theta}(o_{i,t})}{\partial \theta_l} \right\|_2 \leq \|\mathbf{1}_k - p_{i,t}\|_2 b^W b_l^G \prod_{i=l}^L b_i^J$$

We further bound

$$\begin{aligned} \|\mathbf{1}_k - p_{i,t}\|_2 &= \sqrt{(1 - p_{i,t}(k))^2 + \sum_{j \neq k} p_{i,t}(j)^2} \geq 1 - p_{i,t}(k) = 1 - \pi_{\theta}(o_{i,t}). \\ \|\mathbf{1}_k - p_{i,t}\|_2 &= \sqrt{(1 - p_{i,t}(k))^2 + \sum_{j \neq k} p_{i,t}(j)^2} \leq \sqrt{(1 - p_{i,t}(k))^2 + \left(\sum_{j \neq k} p_{i,t}(j) \right)^2} \\ &= \sqrt{(1 - p_{i,t}(k))^2 + (1 - p_{i,t}(k))^2} = \sqrt{2} (1 - p_{i,t}(k)) = \sqrt{2} (1 - \pi_{\theta}(o_{i,t})). \end{aligned}$$

Therefore, we further reach

$$(1 - \pi_\theta(o_{i,t})) a^W a_l^G \prod_{i=l}^L a_i^J \leq \left\| \frac{\partial \log \pi_\theta(o_{i,t})}{\partial \theta_l} \right\|_2 \leq \sqrt{2} (1 - \pi_\theta(o_{i,t})) \|1_k - \pi_\theta(o_{i,t})\|_2 b^W b_l^G \prod_{i=l}^L b_i^J$$

Finally, by noting that

$$\|\nabla_\theta \log \pi_\theta(o_{i,t})\|_2^2 = \sum_{l=1}^L \left\| \frac{\partial \log \pi_\theta(o_{i,t})}{\partial \theta_l} \right\|_2^2,$$

hence leading to

$$\frac{1}{\sqrt{L}} \sum_{l=1}^L \left\| \frac{\partial \log \pi_\theta(o_{i,t})}{\partial \theta_l} \right\|_2 \leq \|\nabla_\theta \log \pi_\theta(o_{i,t})\|_2 \leq \sum_{l=1}^L \left\| \frac{\partial \log \pi_\theta(o_{i,t})}{\partial \theta_l} \right\|_2$$

Finally, we have

$$\|g_{i,t}\|_2 = w_{it} |\gamma_{i,t}| \|\nabla_\theta \log \pi_\theta(o_{i,t})\|_2.$$

Using the bound for $\|\nabla_\theta \log \pi_\theta(o_{i,t})\|_2$ developed above, we reach the conclusion.

To prove the theorem 3.6, we need the following lemma.

Lemma D.2. *Let $v_1, \dots, v_n \stackrel{iid}{\sim} \text{Unif}(\mathbb{S}^{d-1}) \subset \mathbb{R}^d$. There exists universal constants $C, c > 0$ such that for $\delta \in (0, 1)$, with probability at least $1 - \delta$, we have*

$$\max_{i \neq j} |\langle v_i, v_j \rangle| \leq \sqrt{\frac{1}{cd} \log(Cn^2) + \log \frac{1}{\delta}}. \quad (30)$$

Proof. We consider the function $f_u(v) = \langle v, u \rangle$ with $v \in \mathbb{S}^{d-1}$. We are going to apply Levy's lemma to the function f_u .

First, we verify the Lipschitz constraint. For any $v, v' \in \mathbb{S}^{d-1}$, we have

$$|f_u(v) - f_u(v')| = |\langle v - v', u \rangle| \leq \|v - v'\|_2 \|u\|_2 = \|v - v'\|_2,$$

hence $f_u(v)$ is 1-Lipschitz on \mathbb{S}^{d-1} .

It is obvious that $\mathbb{E}_v[\langle v, u \rangle] = 0$ and also $\text{med}(f_u(v)) = 0, v \sim \mathbb{S}^{d-1}$.

Using Levy's lemma, for every $\epsilon > 0$, we have

$$\mathbb{P}(|\langle v, u \rangle| \geq \epsilon) \leq C \exp(-cde^2).$$

From the two-vector result, we have

$$\mathbb{P}(|\langle v_i, v_j \rangle| \geq \epsilon) \leq C \exp(-cd\epsilon^2), \forall i \neq j.$$

This follows that

$$\mathbb{P}(\exists i \neq j : |\langle v_i, v_j \rangle| \geq \epsilon) \leq n^2 C \exp(-cd\epsilon^2).$$

To ensure $n^2 C \exp(-cd\epsilon^2) \leq \delta$, we choose $\epsilon = \sqrt{\frac{1}{cd} (\log(Cn^2) + \log \frac{1}{\delta})}$, leading to

$$\mathbb{P}\left(\max_{i \neq j} |\langle v_i, v_j \rangle| < \epsilon\right) \geq 1 - \delta.$$

□

D.6. Proof of Theorem 3.6

(i) We have

$$\nabla_{\theta} \mathcal{L}_{\mathcal{S}}(\pi_{\theta}) = \mathbb{E}_{\mathcal{S}} \left[\frac{1}{\sum_i^G |o_i|} \sum_{i=1}^G \sum_{t=1}^{|o_i|} g_{i,t} \right].$$

Therefore, we obtain

$$\|\nabla_{\theta} \mathcal{L}_{\mathcal{S}}(\pi_{\theta})\|_2 \leq \mathbb{E}_{\mathcal{S}} \left[\frac{1}{\sum_i^G |o_i|} \sum_{i=1}^G \sum_{t=1}^{|o_i|} \|g_{i,t}\|_2 \right] \leq \mathbb{E}_{\mathcal{S}} \left[\frac{\sqrt{2}}{\sum_i^G |o_i|} \sum_{i=1}^G \sum_{t=1}^{|o_i|} w_{i,t} (1 - \pi(o_{i,t})) U_{i,t} \right].$$

ii) We write the gradient $\nabla_{\theta} \mathcal{L}_{\mathcal{S}}(\pi_{\theta})$ as

$$\nabla_{\theta} \mathcal{L}_{\mathcal{S}}(\pi_{\theta}) = \mathbb{E}_{\mathcal{S}} \left[\frac{1}{\sum_{i=1}^G |o_i|} \sum_{i=1}^G \sum_{t=1}^{|o_i|} g_{i,t} \right] = \frac{1}{|\mathcal{S}|} \sum_{k=1}^N \frac{1}{\sum_{i=1}^G |o_{ki}|} \sum_{i=1}^G \sum_{t=1}^{|o_{ki}|} g_{i,t}^k.$$

This follows that

$$\begin{aligned} \|\nabla_{\theta} \mathcal{L}_{\mathcal{S}}(\pi_{\theta})\|_2^2 &= \frac{1}{|\mathcal{S}|^2} \left\| \sum_{k=1}^N \frac{1}{\sum_{i=1}^G |o_{ki}|} \sum_{i=1}^G \sum_{t=1}^{|o_{ki}|} g_{i,t}^k \right\|_2^2 \\ &= \frac{1}{|\mathcal{S}|^2} \left[\sum_{k=1}^N \sum_{i=1}^G \sum_{t=1}^{|o_{ki}|} \frac{\|g_{i,t}^k\|_2^2}{(\sum_{i=1}^G |o_{ki}|)^2} \right] + \frac{1}{|\mathcal{S}|^2} \sum_{k,k'} \sum_{i,i'} \sum_{t,t'} \frac{1}{(\sum_i |o_{ki}|)(\sum_{i'} |o_{k'i'}|)} \left\langle \frac{g_{i,t}^k}{\|g_{i,t}^k\|}, \frac{g_{i',t'}^{k'}}{\|g_{i',t'}^{k'}\|} \right\rangle \|g_{i,t}^k\| \|g_{i',t'}^{k'}\| \end{aligned}$$

Using Lemma D.2 for $v_{i,t}^k = \frac{g_{i,t}^k}{\|g_{i,t}^k\|}$, we have with probability at least $1 - \delta$, we have

$$\left\langle \frac{g_{i,t}^k}{\|g_{i,t}^k\|}, \frac{g_{i',t'}^{k'}}{\|g_{i',t'}^{k'}\|} \right\rangle \leq \epsilon,$$

with $\epsilon = \sqrt{\frac{1}{cd} (\log(CK^2) + \log \frac{1}{\delta})}$ where $K = \sum_{k=1}^N \sum_{i=1}^G |o_{ki}|$.

This further implies

$$\begin{aligned} \|\nabla_{\theta} \mathcal{L}_{\mathcal{S}}(\pi_{\theta})\|_2^2 &\geq \frac{1}{|\mathcal{S}|^2} \left[\sum_{k=1}^N \left(\frac{1}{(\sum_{i=1}^G |o_{ki}|)^{3/2}} \sum_{i=1}^G \sum_{t=1}^{|o_{ki}|} \|g_{i,t}^k\|_2 \right)^2 \right] - \frac{\epsilon}{|\mathcal{S}|^2} \sum_{k,k'} \sum_{i,i'} \sum_{t,t'} \frac{1}{(\sum_i |o_{ki}|)(\sum_{i'} |o_{k'i'}|)} \|g_{i,t}^k\| \|g_{i',t'}^{k'}\| \\ &\geq \frac{1}{|\mathcal{S}|^2} \left[\frac{1}{|\mathcal{S}|} \left(\sum_{k=1}^N \frac{1}{(\sum_{i=1}^G |o_{ki}|)^{3/2}} \sum_{i=1}^G \sum_{t=1}^{|o_{ki}|} \|g_{i,t}^k\|_2 \right)^2 \right] - \frac{\epsilon}{|\mathcal{S}|^2} \left[\sum_k \sum_i \sum_t \frac{\|g_{i,t}\|}{\sum_i |o_{ki}|} \right] \left[\sum_{k'} \sum_{i'} \sum_{t'} \frac{\|g_{i',t'}\|}{\sum_{i'} |o_{k'i'}|} \right] \\ &\geq \frac{1}{|\mathcal{S}|^2} \mathbb{E}_{\mathcal{S}} \left[\left(\frac{1}{(\sum_{i=1}^G |o_i|)^{3/2}} \sum_{i=1}^G \sum_{t=1}^{|o_i|} \|g_{i,t}\|_2 \right)^2 \right] - \epsilon \mathbb{E}_{\mathcal{S} \times \mathcal{S}} \left[\left(\sum_i \sum_t \frac{\|g_{i,t}\|}{\sum_i |o_i|} \right) \left(\sum_{i'} \sum_{t'} \frac{\|g_{i',t'}\|}{\sum_{i'} |o_{i'}|} \right) \right] \end{aligned}$$

Finally, using the upper and lower bounds of $\|g_{i,t}\|_2$, we gain

$$\begin{aligned} \|\nabla_{\theta} \mathcal{L}_{\mathcal{S}}(\pi_{\theta})\|_2^2 &\geq \frac{1}{|\mathcal{S}|^2} \mathbb{E}_{\mathcal{S}} \left[\left(\sum_{i=1}^G \sum_{t=1}^{|o_i|} \frac{w_{i,t} (1 - \pi_{\theta}(o_{i,t})) L_{i,t}}{(\sum_{i=1}^G |o_i|)^{3/2} \sqrt{L}} \right)^2 \right] \\ &\quad - 2\epsilon \mathbb{E}_{\mathcal{S} \times \mathcal{S}} \left[\left(\sum_{i=1}^G \sum_{t=1}^{|o_i|} \frac{w_{i,t} (1 - \pi_{\theta}(o_{i,t})) L_{i,t}}{\sum_i |o_i|} \right) \left(\sum_{i=1}^G \sum_{t=1}^{|o'_i|} \frac{w'_{i,t} (1 - \pi_{\theta}(o'_{i,t})) L'_{i,t}}{\sum_{i'} |o'_i|} \right) \right]. \end{aligned}$$